Electron-Hole-Phonon Transport in Dirac Materials

A thesis written for the degree of MSc Theoretical Physics by
Klas Sjöstedt

Supervisor: Assoc. Prof. Dr. Lars Fritz

Institute for Theoretical Physics, Faculty of Science
Buys Ballotgebouw
Universiteit Utrecht
Princetonplein 5, 3584CC
Utrecht

July, 2022

Universiteit Utrecht

Acknowledgements

Strange, how a phone call can change your day,
take you away–
away from the feeling of being alone
Bless the telephone
-Labi Siffre, *Bless the Telephone*

Starting a master's programme during an ongoing global pandemic certainly had its fair share of downsides. Although I met some wonderful people here in the Netherlands, it was inevitable to feel alone and isolated amidst online lectures, curfews and even restrictions on the numbers of visitors allowed in my apartment. I am lucky to live in a time where speaking over the phone, and by extension video calling, has never been easier, and to have people around me checking in regularly. I am grateful for my family, my friends back in Sweden, my friends here in Utrecht, the members of the VUSO orchestra, and the research group of Lars Fritz and Dirk Schuricht, for keeping me off the cycle of eating, sleeping and studying in the same room.

More concretely, I am thankful for having had Lars Fritz as the supervisor for this master's thesis project. He has had endless patience for my many questions, as well as words of reassurance when I have expressed doubts about the validity of methods or formalities regarding the project. On top of this, his willingness to make time for meetings and to discuss physics has been immensely appreciated, and I have received much valuable feedback on both physics as well as academic speaking and writing. For anyone looking for a potential supervisor, I cannot recommend him enough.

For Swedish-speaking readers, I have added a Sammanfattning on the next page, below the usual Abstract.

Abstract

Hydrodynamics is one of the few theories available to study macroscopically many-body systems which are out-of-equilibrium and not necessarily weakly interacting. Moreover, quantum particles can also have a hydrodynamic description, provided the length and time scales probed are long enough. This opens up for the study of exotic condensed matter systems, where assumptions of e.g. negligible electron-electron interactions are no longer justified. One particularly promising candidate to apply this theory to is *graphene*, an atomically thin layer of carbon atoms arranged in a honeycomb structure. In 2004, graphene was the first found example of a two-dimensional crystal, and it falls under the more general class of *Dirac materials*. These materials share universal "relativistic" features making them strikingly different from, for instance, ordinary metals. In this thesis, the framework of the *Boltzmann equation* is derived, and from it a transport theory can be setup. Then, Dirac materials are presented, and graphene is singled out as an intriguing candidate to observe electron hydrodynamics in. Finally, two models for graphene are developed. The first considers only electrons and holes, and the second improves upon this by also including phonons. The electrical conductivity σ and thermal conductivity κ are derived from each model, and the results are discussed in regards to earlier theoretical findings. In particular, the so-called minimal electrical conductivity for graphene is reproduced, and the expression for its thermal conductivity provides insight into the transport properties of general Dirac materials.

Sammanfattning

Hydrodynamik är en av få teorier tillgängliga för att studera system med makroskopiskt många partiklar, som dessutom är utom jämvikt och inte nödvändigtvis svagt interagerande. Dessutom kan kvantmekaniska partiklar ges en hydrodynamisk beskrivning, givet att de längd- och tidsskalor som studeras är långa nog. Detta möjliggör studier av exotisk kondenserad materia, där antagelser som t.ex. försumbara elektron-elektron-interaktioner inte längre är försvarbara. En särskilt lovande kandidat att tillämpa denna teori på är *grafen*, ett atomärt tunnt skikt av kolatomer arrangerade i en vaxkakeliknande struktur. 2004 blev grafen det första funna exemplet på en tvådimensionell kristall, och det faller under den mer allmänna klassen av *Diracmaterial*. Dessa material delar universala "relativistiska" egenskaper som gör dem slående annorlunda gentemot bland annat vanliga metaller. I denna uppsats härleds ramverket kring *Boltzmannekvationen*, och från detta kan en transportteori etableras. Därefter presenteras Diracmaterial, och särskilt grafen pekas ut som en fascinerande kandidat för att observera elektronhydrodynamik. Slutligen utvecklas två modeller för grafen. Den första behandlar enbart elektroner och hål, och den andra förbättras genom att även inludera fononer. Den elektriska ledningsförmågan σ och värmeledningsförmågan κ härleds från båda modeller, och resultaten diskuteras i förhållande till tidigare teoretiska upptäckter. I synnerhet återskapas den så kallade minimala elektriska ledningsförmågan hos grafen, och uttrycket för dess värmeledningsförmåga ger insikt i transportegenskaper hos allmänna Diracmaterial.

Contents

1 Introduction

Hydrodynamics is the description of the flow of fluids, and as such tries to capture the behaviour of materials when they are modelled as continuous matter, rather than as discrete particles. This framework is highly successful in describing everyday fluids, such as water or honey, but also matter not conventionally thought of as fluids. For instance, the modelling of galaxy formation [1], simulations of the Earth's tectonic plate motion [2], and the study of the motions of crowds at heavy metal concerts [3] have all been done using a fluid dynamics description. Clearly, hydrodynamics is applicable also in cases where the constituents that make up the "fluid" are not "particles" in the usual sense.

A continuum description of matter can be expected to be valid for any class of discrete particles (or "particles"), provided the length scales considered are much longer than the length scale set by the particles, i.e. their mean free path ℓ. For this reason, hydrodynamic descriptions of quantum particles are also possible, which allows for e.g. the modelling of charge carriers in condensed matter systems. In particular, when there are no non-interacting quasiparticle descriptions available, hydrodynamics remains a powerful tool to study macroscopic properties of the system, such as transport phenomena.

Another enticing aspect of a hydrodynamic description is that it is non-perturbative in particle interaction strengths. Thus it is applicable to, among others, systems where the conventional methods of condensed matter theory [4] fail. For instance, hydrodynamic descriptions are still available for non-Fermi liquids, also called "strange" metals, which opens up for a study of transport theory in a broader class of materials.

One class of such materials is Dirac materials, in which the emergent quasiparticles have "relativistic" properties by virtue of their dispersions. These properties include anomalous transport behaviour such as the absence of back scattering, leading to quantum tunneling through arbitrarily high and wide potentials, a phenomenon known as the Klein paradox [5]. Other aspects include universal power laws of thermodynamic response functions, separating them from e.g. conventional metals, and Zitterbewegung, or "jittery motion". Moreover, these universal properties are typically protected by symmetries, more readily allowing for experimental verification of theoretical findings. In particular, graphene has received much attention over the last two decades for its many unusual properties. It was the first experimentally discovered two-dimensional crystal [6], and consists of a single layer of carbon atoms arranged in a honeycomb lattice. It turns out that graphene is also an excellent setting to study electron hydrodynamics in.

This thesis is structured in the following way: firstly, the Boltzmann equation is discussed in Section 2. This equation is a powerful to study transport in many-body systems, particularly when the particles are strongly interacting. Next, Section 3 is devoted to transport theory, and how such a theory can be set up from the formalism of the Boltzmann equation. After this, Dirac materials are presented in Section 4, together with many of the features that distinguish them from e.g. conventional metals. Graphene is also discussed in more detail, and its suitability for observing electron hydrodynamics is motivated. In Section 5, a first model for graphene is developed, accounting for electrons and holes. After introducing an approximation scheme based on the so-called relaxation time approximation, the resulting transport coefficients are found. After this, the model is made more accurate by also including phonons in he description in Section 6, and the resulting transport coefficients are compared. Lastly, an outlook of the thesis is provided in Section 7, as well as a summary in Section 8. A few somewhat lengthy derivations are also relegated to the two Appendices A and B.

2 The Boltzmann Equation

For a continuum treatment of matter, an equation for the distribution of the particles is needed. The distribution that will be used is the *one-body distribution* $f = f(\mathbf{r}, \mathbf{p}, t)$, which is defined such that

$$f(\mathbf{r}, \mathbf{p}, t)\mathrm{d}^d r \mathrm{d}^d p$$

gives the average number of particles found within $\mathrm{d}^d r$ of position $\mathbf{r}$, within $\mathrm{d}^d p$ of momentum $\mathbf{p}$, at time t. Here, d denotes the dimensionality of the system, which will almost always be $d = 2$ for the systems considered in this work.

The equation in f that describes the dynamics of the system is the *Boltzmann equation*. Its heuristic derivation starts from considering the total time derivative of the distribution, $\frac{\mathrm{d}f}{\mathrm{d}t}$. If the constituent particles are non-interacting, Liouville's theorem of classical mechanics applies, and the distribution function must be constant along phase space paths of the particles. The derivative must then vanish, resulting in

$$\frac{\mathrm{d}f}{\mathrm{d}t} = \frac{\partial f}{\partial t} + \frac{\partial \mathbf{r}}{\partial t} \cdot \frac{\partial f}{\partial \mathbf{r}} + \frac{\partial \mathbf{p}}{\partial t} \cdot \frac{\partial f}{\partial \mathbf{p}} = 0 \tag{1}$$

Here, $\frac{\mathrm{d}f}{\mathrm{d}t}$ refers to taking the time derivative along the phase space path of a given particle. Therefore, $\frac{\partial \mathbf{r}}{\partial t}$ and $\frac{\partial \mathbf{p}}{\partial t}$ are governed by the equations of motion of the particles, and we may write $\mathbf{v} = \frac{\partial \mathbf{r}}{\partial t}$ for the velocity of a particle, as well as $\mathbf{F}^{\text{ext}} = \frac{\partial \mathbf{p}}{\partial t}$ for the total external force acting on a particle.

If collisions between particles are present, however, it is not generally true that $\frac{\mathrm{d}f}{\mathrm{d}t}$ vanishes. This is since collisions allow for momentum exchange between particles, which may alter the distribution over time as the system strives for equilibrium. The equation is modified to account for this by adding a term to the right-hand side, such that

$$\frac{\partial f}{\partial t} + \mathbf{v} \cdot \frac{\partial f}{\partial \mathbf{r}} + \mathbf{F}^{\text{ext}} \cdot \frac{\partial f}{\partial \mathbf{p}} = \mathcal{C}[f] \tag{2}$$

Here, $\mathcal{C}[f]$ is called the *collision integral*, and is in general a functional in f (it is, in itself, also a function in $\mathbf{r}, \mathbf{p}, t$). The exact form of $\mathcal{C}$ will vary depending on the system in question, and in particular on which collision events occur in the system. Some of its properties will be investigated in section 2.1.

Equation (2) is the Boltzmann equation, derived for classical particles. The extension to quantum particles is discussed in section 2.2. Due to the functional dependence of the collision integral on f, it is generally an *integro-differential equation*, meaning analytical solutions are usually impossible to find. The exception is when the system is in thermodynamic equilibrium, in which case both sides of the equation vanish. For classical particles, f would then correspond a Boltzmann distribution of the form

$$f(\mathbf{p}) = \exp\left(-\frac{\epsilon(\mathbf{p}) - \mu - \mathbf{p} \cdot \mathbf{V}}{k_B T}\right) \tag{3}$$

where k_B is Boltzmann's constant, T is the temperature, ϵ is the single-particle dispersion, μ is the chemical potential, and $\mathbf{V}$ is a bulk flow parameter. The latter allows for the fluid to move uniformly at constant speed, which by galilean invariance is equivalent to being at rest. In the quantum case, instead, f would be either a Fermi-Dirac or a Bose-Einstein distribution:

$$f(\mathbf{p}) = \left(\exp\left(\frac{\epsilon(\mathbf{p}) - \mu - \mathbf{p} \cdot \mathbf{V}}{k_B T}\right) \pm 1\right)^{-1} \tag{4}$$

Here, the upper sign refers to fermions, and the lower to bosons. Section 2.3 will describe a relaxation of the notion of equilibrium, and in turn generalisations of the aforementioned distributions. Finally, an approximation scheme for the collision integral is discussed in Section 2.4, resulting in a drastic simplification of the Boltzmann equation.

2.1 The Collision Integral

As mentioned above, the collision integral $\mathcal{C}[f]$ is system-specific, and will in particular depend on what types of scattering processes occur. Specifically, the number of ingoing and outgoing particles in a given scattering process determines the exact form of $\mathcal{C}[f]$. Usually, particle number conservation is assumed, in which case the numbers of ingoing and outgoing particles must be equal. Still, this leaves an infinite number of possible processes open; there could be 1-body scattering due to an external potential, or 2-body scattering where two particles collide and exchange momenta, or generally n-body processes for any natural number n. For simplicity, only 2-body scattering will be considered, since they elucidate all of the key properties investigated below. Similarly, point particles are assumed for convenience, meaning there is no need to consider angular momentum exchange in the scattering processes. Finally, conservation of momentum and energy is assumed for the collisions in this section.

For 2-body scattering of classical particles (and similarly for general n-body scattering), the collision integral can be constructed based on heuristic arguments. The discussion presented below closely follows that of Lifshitz and Pitaevskii [7]. To start off, consider two particles colliding at position $\mathbf{r}$ at time t; one with ingoing momentum within $\mathrm{d}^d p$ of $\mathbf{p}$ and the other within momentum $\mathrm{d}^d p_1$ of $\mathbf{p}_1$. Suppose they then scatter such that one particle ends up with momentum within $\mathrm{d}^d p'$ of $\mathbf{p}'$ and the other within $\mathrm{d}^d p'_1$ of $\mathbf{p}'_1$. Now, the total number of collisions (per unit volume and per unit time) of this kind must be proportional to the number of molecules with momentum $\mathbf{p}$, which is $f(\mathbf{r}, \mathbf{p}, t)\mathrm{d}^d p$. Similarly, the number of collisions must be proportional to $f(\mathbf{r}, \mathbf{p}_1, t)\,\mathrm{d}^d p_1$. Finally, the collision rate should be proportional to the ranges $\mathrm{d}^d p'$ and $\mathrm{d}^d p'_1$. All in all, the probability can then be written

$$w(\mathbf{p}', \mathbf{p}'_1 | \mathbf{p}, \mathbf{p}_1)\, f(\mathbf{r}, \mathbf{p}, t)\, f(\mathbf{r}, \mathbf{p}_1, t)\, \mathrm{d}^d p' \mathrm{d}^d p'_1 \mathrm{d}^d p \mathrm{d}^d p_1$$

so that the function w carries all the information about the specifics of the collisions. Here, the order in which the arguments of w are written follows the conventions of quantum mechanics, with final states written on the left and initial states on the right. Figure 1 shows a schematic of such a process.

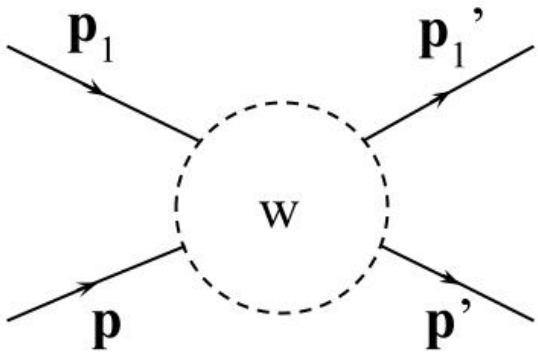

Figure 1: Generic 2-body scattering with ingoing momenta $\mathbf{p}$ and $\mathbf{p}_1$ on the left, and outgoing momenta $\mathbf{p}'$ and $\mathbf{p}_1'$ on the right. The specifics of the collision is captured by $w = w\left(\mathbf{p}', \mathbf{p}_1' | \mathbf{p}, \mathbf{p}_1\right)$.

The function w must generally be calculated from first principles, but it is nonetheless possible to write down the collision integral in terms of it. Also, to be fully precise, the two-body distribution should be used instead of the product of one-body distributions above, but in the low-density limit this factorisation is valid. Moreover, this ensures the closure of the Boltzmann equation.

To arrive at the collision integral, there are two kinds of processes to consider. Firstly, particles initially outside of momentum $\mathbf{p}$ may scatter into this momentum. This would increase the distribution $f(\mathbf{r}, \mathbf{p}, t)$ over time, and these processes could be referred to as "gains". Secondly, particles initially with momentum $\mathbf{p}$ may scatter out of this momentum state. This would conversely decrease $f(\mathbf{r}, \mathbf{p}, t)$ with time, and these processes may analogously be called "losses". In terms of the 2-body collision events above, the collision integral can then be written

$$\begin{aligned} \mathcal{C}[f] = &\int \mathrm{d}^d p_1 \mathrm{d}^d p' \mathrm{d}^d p_1' \; w\left(\mathbf{p}, \mathbf{p}_1 | \mathbf{p}', \mathbf{p}_1'\right) f' f_1' \\ &- \int \mathrm{d}^d p_1 \mathrm{d}^d p' \mathrm{d}^d p_1' \; w\left(\mathbf{p}', \mathbf{p}_1' | \mathbf{p}, \mathbf{p}_1\right) f f_1 \end{aligned} \tag{5}$$

where, for brevity, the arguments of f are suppressed, and the indices are used to indicate which momentum state f is being evaluated on; for instance, $f_1 = f(\mathbf{r}, \mathbf{p}_1, t)$ and $f' = f(\mathbf{r}, \mathbf{p}', t)$.

Even without knowledge of the exact scattering process, and therefore w, a few conclusions can still be drawn by requiring two symmetries. The first is time reversal symmetry, which must hold for classical and quantum particles alike. Denoting time reversal by a superscript T, it follows that $\mathbf{r}^T = \mathbf{r}$, while $\mathbf{p}^T = -\mathbf{p}$ and $t^T = -t$. In equilibrium, detailed balance asserts that

$$w\left(\mathbf{p}', \mathbf{p}_1' | \mathbf{p}, \mathbf{p}_1\right) f^0 f^0{}_1 \mathrm{d}^d p' \mathrm{d}^d p_1' \mathrm{d}^d p \mathrm{d}^d p_1 = w\left(\mathbf{p}^T, \mathbf{p}_1^T | \mathbf{p}'^T, \mathbf{p}_1'^T\right) f^{0'^T} f^{0'^T}_1 \mathrm{d}^d p' \mathrm{d}^d p_1' \mathrm{d}^d p \mathrm{d}^d p_1 \tag{6}$$

denoting an equilibrium distribution by f^0. Now, the phase space volume element $\mathrm{d}^d p' \mathrm{d}^d p_1' \mathrm{d}^d p \mathrm{d}^d p_1$ remains unchanged under time reversal. Moreover, the particle energy is invariant under time reversal, so that $f^0(\mathbf{p}^T) = f^0(\mathbf{p})$. Finally, conservation of momentum and energy ensure that

$$f_1^0 f^0{}_1 = f^{0'^T} f^{0'^T}_1 \tag{7}$$

These relations reduce (6) to

$$w\left(\mathbf{p}', \mathbf{p}_1' | \mathbf{p}, \mathbf{p}_1\right) = w\left(\mathbf{p}^T, \mathbf{p}_1^T | \mathbf{p}'^T, \mathbf{p}_1'^T\right) \tag{8}$$

The other symmetry to consider is parity symmetry, which again ought to hold for classical and quantum particles, provided they are pointlike. Denoting the parity inversion by a superscript P, it follows that $\mathbf{r}^P = -\mathbf{r}$ and $\mathbf{p}^P = -\mathbf{p}$ while $t^P = t$. By similar arguments as for the time reversal case, it is found that

$$w\left(\mathbf{p}', \mathbf{p}_1' | \mathbf{p}, \mathbf{p}_1\right) = w\left(\mathbf{p}^P, \mathbf{p}_1^P | \mathbf{p}'^P, \mathbf{p}_1'^P\right) \tag{9}$$

In particular, requiring both symmetries to hold simultaneously, the two relations combine to give

$$w\left(\mathbf{p}', \mathbf{p}_1' | \mathbf{p}, \mathbf{p}_1\right) = w\left(\mathbf{p}^{PT}, \mathbf{p}_1^{PT} | \mathbf{p}'^{PT}, \mathbf{p}_1'^{PT}\right) \tag{10}$$

As each symmetry operation changes the sign of $\mathbf{p}$ once, the combination leaves the sign of any momentum unchanged, resulting in

$$w\left(\mathbf{p}', \mathbf{p}_1' | \mathbf{p}, \mathbf{p}_1\right) = w\left(\mathbf{p}, \mathbf{p}_1 | \mathbf{p}', \mathbf{p}_1'\right) \tag{11}$$

For point particles, then, detailed balance implies that each process is exactly balanced by its reverse. Using the above relation, the expression for the collision integral from (5) shortens to

$$\mathcal{C}[f] = \int \mathrm{d}^d p_1 \mathrm{d}^d p' \mathrm{d}^d p_1' \; w\left(\mathbf{p}, \mathbf{p}_1 | \mathbf{p}', \mathbf{p}_1'\right) \left(f' f_1' - f f_1\right) \tag{12}$$

This form of the collision integral is then the most general one that satisfies all the symmetry relations and conservation laws imposed above, provided only 2-body scattering events take place. A key feature which is now readily shown is that the collision integral vanishes when evaluated over an equilibrium distribution:

$$\begin{aligned} \mathcal{C}\left[f^0\right] &= \int \mathrm{d}^d p_1 \mathrm{d}^d p' \mathrm{d}^d p_1' \; w\left(\mathbf{p}, \mathbf{p}_1 | \mathbf{p}', \mathbf{p}_1'\right) \left(f^{0\prime} f^{0\prime}{}_1 - f^0 f^0{}_1\right) \\ &= 0 \end{aligned} \tag{13}$$

This, like before, follows from momentum and energy conservation, so that

$$f^0 f_1^0 = f^{0\prime} f^{0\prime}{}_1 \tag{14}$$

At this point, it should again be stressed that other n-body processes could be considered. However, it can be shown that they all share the properties discussed above, and the expression for the collision integral generalises in a natural way; for instance, for 3-body processes it is found that

$$\mathcal{C}[f] = \int \mathrm{d}^d p_1 \mathrm{d}^d p_2 \mathrm{d}^d p' \mathrm{d}^d p_1' \mathrm{d}^d p_2' \; w\left(\mathbf{p}, \mathbf{p}_1, \mathbf{p}_2 | \mathbf{p}', \mathbf{p}_1', \mathbf{p}_2'\right) \left(f' f_1' f_2' - f f_1 f_2\right) \tag{15}$$

2.2 From Classical to Semiclassical

While the Boltzmann equation formalism is able to incorporate some aspects of quantum physics, there are a few it cannot, and it is to be thought of as a semiclassical treatment when applied to particles with quantum statistics. For instance, the Pauli exclusion principle is upheld by fermions, as is discussed later in this section. However, since the Boltzmann equation framework fundamentally treats position and momentum as independent variables, the Heisenberg uncertainty principle cannot be captured. Moreover, for the Boltzmann equation to be applicable it is necessary to consider length scales much longer than the de Broglie wavelengths of the (quasi-)particles in question, in addition to the normal requirement of considering length scales much longer than their mean free path.

To adhere to the conventions of quantum mechanics, the wave vector $\mathbf{k}$ of a particle will be preferred over its momentum $\mathbf{p}$, with the two related by $\mathbf{p} = \hbar\mathbf{k}$. For convenience, units will then be used such that $\hbar = 1$ for most of the calculations, but missing factors will be restored using dimensional analysis when key results are presented.

While the left-hand side of the Boltzmann equation (2) remains the same for quantum particles, the collision integral (12) derived for classical particles will change. Formally, the collision integral must be derived from the underlying theory of the so-called Schwinger-Keldysh formalism, which is a general framework for studying out-of-equilibrium quantum systems. From this formalism, the collision integral corresponding to any collision process can be derived, but the theory is beyond the scope of this thesis. Instead, it will be noted that the collision integral takes the form [8]

$$\mathcal{C}[f] = \int \frac{\mathrm{d}^d k_1}{(2\pi)^d} \frac{\mathrm{d}^d k'}{(2\pi)^d} \frac{\mathrm{d}^d k_1'}{(2\pi)^d} \, w\left(\mathbf{k}, \mathbf{k}_1 | \mathbf{k}', \mathbf{k}_1'\right) \left\{ f' f_1' \left(1 \mp f\right)\left(1 \mp f_1\right) - f f_1 \left(1 \mp f'\right)\left(1 \mp f_1'\right) \right\} \tag{16}$$

for 2-body scattering events. As before, the upper signs correspond to fermions, and the lower to bosons. For fermions, the added factors of $1 - f$ have a natural interpretation; the probability of a fermion scattering into momentum $\mathbf{k}$ should be proportional to $1 - f$, which is precisely the probability that the state is not already occupied by another fermion. Thus, the added factors reflect the Pauli exclusion principle. For bosons, the probability interpretation of the added factors fails, but nonetheless it is seen that the factors of $1 + f$ enhance scattering into states already occupied by other bosons, which agrees with physical intuition.

Much like in the previous section, the collision integral vanishes when evaluated over an equilibrium distribution, i.e. either the Fermi-Dirac or the Bose-Einstein distribution:

$$\mathcal{C}\left[f^0\right] = 0 \tag{17}$$

This again follows from momentum and energy conservation, together with noting that

$$\frac{f^0}{1 \mp f^0} = \exp\left(\frac{\epsilon(\mathbf{k}) - \mu - \mathbf{k} \cdot \mathbf{V}}{k_B T}\right) \tag{18}$$

returns the Boltzmann distribution.

2.3 Local Equilibrium

In the usual definition of a thermodynamic equilibrium, it is required that the temperature T is constant throughout a material. Similarly, the chemical potential μ must be constant, and the bulk flow profile $\mathbf{V}$ must be uniform. As discussed earlier, the distributions corresponding to such an equilibrium are the Boltzmann, Fermi-Dirac, or Bose-Einstein distributions, depending on the nature of the particles.

In the Boltzmann equation formalism, it is useful to define a second, more relaxed kind of equilbrium, called *local equilibrium*. A local equilibrium resembles a thermodynamic equilibrium (which could be contrasted as a "global" equilibrium), but the temperature, chemical potential, and bulk flow velocity are allowed to vary in space and/or time. In this way, the system behaves locally and for short times as if it were in thermodynamic equilibrium, but on larger scales it does not. Such a setting is natural to consider when investigating strongly interacting systems, which tend to thermalise rapidly in such a way as to yield local equilibrium distributions.

Formally, the above procedure corresponds to writing $T = T(\mathbf{r}, t)$, $\mu = \mu(\mathbf{r}, t)$, and $\mathbf{V} = \mathbf{V}(\mathbf{r}, t)$. For the Boltzmann equation to be applicable, it is necessary that these quantities vary over length scales much longer than the mean free path of the particles, and over time scales much longer than

their mean free time. Strictly speaking, quantities like temperature are only well-defined in the context of thermodynamic equilibrium, but such a discussion is beyond the scope of this work. The reader is referred to chapter 4 of [9] for a nuanced discussion on the matter.

Corresponding to a local equilibrium are distributions f^0, again depending on the statistics of the particles. Taking quantum particles, the relevant distribution takes the form

$$f^0(\mathbf{r},\mathbf{k},t) = \left(\exp\left(\frac{\epsilon(\mathbf{k}) - \mu(\mathbf{r},t) - \mathbf{k}\cdot\mathbf{V}(\mathbf{r},t)}{k_B T(\mathbf{r},t)}\right) \pm 1\right)^{-1} \tag{19}$$

with the top sign for fermions and the bottom for bosons. Thus, the distribution functionally has the form of either a Fermi-Dirac or a Bose-Einstein distribution, except the fields that enter it may vary in space and/or time.

Much like thermodynamic equilibrium, local equilibrium distributions have the property that the collision integral vanishes when evaluated over them. Intuitively, this is reasonable since the system locally appears to be in equilibrium, so that collisions taking place at points have the same backwards and forwards scattering rates. Formally, since the collisions are assumed to occur at points and the fields are slowly varying, detailed balance ensures that the scattering rates into and out of any given momentum state exactly cancel. However, unlike in the thermodynamic case, a local equilibrium distribution is *not* a solution to the Boltzmann equation (2). This is since the left-hand side contains derivatives which are generally non-zero do to the variations of the fields, while the right-hand side contains the vanishing collision integral. To solve the equation, a deviation δf from a local equilibrium must be added, such that

$$f = f^0 + \delta f \tag{20}$$

Given the local equilibrium distribution f^0, which is usually known in, say, an experimental setting where the temperature gradient and flow profile are controlled, the Boltzmann equation thus becomes an equation in the new unknown, δf.

In particular, this scheme provides a way to do perturbative analysis around a local equilibrium distribution. Supposing the deviation δf is small, its contributions to the left-hand side of the Boltzmann equation may be neglected. That is, provided $\delta f \ll f^0$,

$$\frac{\partial f}{\partial \mathbf{r}} \approx \frac{\partial f^0}{\partial \mathbf{r}} \tag{21a}$$

$$\frac{\partial f}{\partial \mathbf{k}} \approx \frac{\partial f^0}{\partial \mathbf{k}} \tag{21b}$$

Regarding the temporal derivative, a steady-state local equilibrium will be assumed in the rest of this work, so that

$$\frac{\partial f}{\partial t} = \frac{\partial \delta f}{\partial t} \tag{22}$$

The two relations (21) are particularly useful because the derivatives of f^0 can be written in terms of derivatives of the fields, as well as the dispersion. For the spatial derivative, it is found that

$$\frac{\partial f^0}{\partial \mathbf{r}} = \left(-\nabla\mu - \mathbf{k}\nabla\cdot\mathbf{V} - \frac{\epsilon - \mu - \mathbf{k}\cdot\mathbf{V}}{T}\nabla T\right)\frac{\partial f^0}{\partial \epsilon} \tag{23}$$

Instead for the momentum derivative,

$$\frac{\partial f^0}{\partial \mathbf{k}} = (\mathbf{v} - \mathbf{V})\frac{\partial f^0}{\partial \epsilon} \tag{24}$$

Now, in the Boltzmann equation the spatial derivative term appears in the form $\mathbf{v} \cdot \frac{\partial f}{\partial \mathbf{r}}$. Therefore, combining the above relations,

$$\begin{aligned}
\mathbf{v} \cdot \frac{\partial f}{\partial \mathbf{r}} &= \left(-\nabla\mu - \mathbf{k}\nabla \cdot \mathbf{V} - \frac{\epsilon - \mu - \mathbf{k} \cdot \mathbf{V}}{T} \nabla T \right) \cdot \left(\mathbf{v} \frac{\partial f^0}{\partial \epsilon} \right) \\
&= \left(-\nabla\mu - \mathbf{k}\nabla \cdot \mathbf{V} - \frac{\epsilon - \mu - \mathbf{k} \cdot \mathbf{V}}{T} \nabla T \right) \cdot \left(\frac{\partial f^0}{\partial \mathbf{k}} + \mathbf{V} \frac{\partial f^0}{\partial \epsilon} \right) \\
&= \left(-\nabla\mu - \mathbf{k}\nabla \cdot \mathbf{V} - \frac{\epsilon - \mu - \mathbf{k} \cdot \mathbf{V}}{T} \nabla T \right) \cdot \frac{\partial f^0}{\partial \mathbf{k}} \\
&\quad + \left(-\mathbf{V} \cdot \nabla\mu - (\mathbf{V} \cdot \mathbf{k})\nabla \cdot \mathbf{V} - \frac{\epsilon - \mu - \mathbf{k} \cdot \mathbf{V}}{T} \mathbf{V} \cdot \nabla T \right) \frac{\partial f^0}{\partial \epsilon}
\end{aligned} \tag{25}$$

This expression can be simplified in a so-called *linear response* regime. Here, any applied external fields, such as an electric field $\mathbf{E}$ or a thermal gradient ∇T, are assumed small, and it follows that all of the quantities $\nabla\mu$, $\mathbf{V}$, $\nabla \cdot \mathbf{V}$ and ∇T are small. Therefore, since the second term of the last line above is quadratic in these terms, it is negligible in comparison to the first, and

$$\mathbf{v} \cdot \frac{\partial f^0}{\partial \mathbf{r}} \approx \left(-\nabla\mu - \mathbf{k}\nabla \cdot \mathbf{V} - \frac{\epsilon - \mu - \mathbf{k} \cdot \mathbf{V}}{T} \nabla T \right) \cdot \frac{\partial f^0}{\partial \mathbf{k}} \tag{26}$$

in the linear response regime. All in all, the Boltzmann equation currently reads

$$\frac{\partial \delta f}{\partial t} + \left(-\nabla\mu - \mathbf{k}\nabla \cdot \mathbf{V} - \frac{\epsilon - \mu - \mathbf{k} \cdot \mathbf{V}}{T} \nabla T + \mathbf{F}^{\text{ext}} \right) \cdot \frac{\partial f^0}{\partial \mathbf{k}} = \mathcal{C}\left[f^0 + \delta f \right] \tag{27}$$

This equation will provide the basis for the development of the models in Sections 5 and 6.

2.4 The Relaxation Time Approximation

As noted earlier in section 2, due to the integro-differential nature of the Boltzmann equation, exact solutions are usually impossible to find outside of thermodynamic equilibrium. For this reason, approximate methods to solve the equation are of great significance to gain theoretical insight. One such method is the so-called *relaxation time approximation* [10], where all the specifics of the collision integral are captured by a single *relaxation time* τ. This time scale would be related to the mean free path ℓ of the particles via

$$\ell = \overline{v}\tau \tag{28}$$

with $\overline{v}$ the average speed of the particles. With the relaxation time introduced, the collision integral is approximated as

$$\mathcal{C}[f] \approx -\frac{\delta f}{\tau} \tag{29}$$

where δf, like in the previous section, measures the deviation of the distribution from (a local or thermodynamic) equilibrium. By this approximation scheme, the collision integral no longer reflects the specifics of the collision processes, such as the number of ingoing and outgoing particles, but rather its overall impact on the equilibration of the particles. In principle, the relaxation time τ could be momentum-dependent, but in the simplest case it is a constant. Immediately, this transforms the Boltzmann equation into a differential equation, i.e. there are no longer integrals

over the distribution present, drastically reducing its complexity. In addition, this somewhat crude approximation still captures a few key features of the full collision integral. Firstly, it expresses the fact that collisions make the system tend to equilibrium, and in this case the equilibration occurs at the fixed rate $\nu = \frac{1}{\tau}$. Moreover, the collision integral vanishes when evaluated on an equilibrium distribution, i.e. $\mathcal{C}\left[f^0\right]$, as must be required.

There is, however, a major drawback of this approximation method, which has been known [11] for as long as the approximation method has been; the form of the collision integral in (29) will, in general, violate the conservation laws normally preserved by collisions. This is most easily seen for a homogeneous distribution f (so that $\frac{\partial f}{\partial \mathbf{r}} = \mathbf{0}$), in the absence of external forces. Then, the Boltzmann equation reads

$$\frac{\partial \delta f}{\partial t} = -\frac{\delta f}{\tau} \tag{30}$$

with the solution

$$\delta f(\mathbf{r}, \mathbf{p}, t) = \delta f(\mathbf{r}, \mathbf{p}, 0) e^{-t/\tau} \tag{31}$$

For instance, then, an excess particle density relaxes to its equilibrium value at the rate $\frac{1}{\tau}$, resulting in a decrease of the total particle number over time. This renders the relaxation time approximation undesirable when conservation laws are upheld by the collision processes considered. Later in this thesis, when the explicit models are introduced in Sections 5 and 6, two improved approximation schemes are developed, guided by the goal of preserving conserved quantities in the system. Developments in this direction have only recently been made in other works [12, 13].

3 Transport Theory

In the framework of the Boltzmann equation, it is straightforward to setup a transport theory, by means of various integrals over momentum of the distribution f. Firstly, the particle number density n is given by

$$n(\mathbf{r}, t) = \int \frac{\mathrm{d}^d k}{(2\pi)^d} \; f \tag{32}$$

Similarly, the momentum density $\mathbf{n}^k$ and energy density n^ϵ are found as

$$\mathbf{n}^k(\mathbf{r}, t) = \int \frac{\mathrm{d}^d k}{(2\pi)^d} \; \mathbf{k} f \tag{33a}$$

$$n^\epsilon(\mathbf{r}, t) = \int \frac{\mathrm{d}^d k}{(2\pi)^d} \; \epsilon f \tag{33b}$$

For brevity, the spatial and temporal arguments will be omitted from now on, in the case that functions are obtained as integrals over momentum.

Next, the particle current density $\mathbf{j}$ and the energy current density $\mathbf{j}^\epsilon$ are given by

$$\mathbf{j} = \int \frac{\mathrm{d}^d k}{(2\pi)^d} \; \mathbf{v} f \tag{34a}$$

$$\mathbf{j}^\epsilon = \int \frac{\mathrm{d}^d k}{(2\pi)^d} \; \epsilon \mathbf{v} f \tag{34b}$$

If the particles are also charged, a particle current naturally gives rise to an electric current $\mathbf{j}^{\text{el}}$. This is given by

$$\mathbf{j}^{\text{el}} = q\mathbf{j} = \int \frac{\mathrm{d}^d k}{(2\pi)^d}\, q\mathbf{v} f \tag{35}$$

if the particles have charge q. Similarly, the particle and energy currents together induce a heat current $\mathbf{j}^q$, related to those currents as

$$\mathbf{j}^q = \mathbf{j}^\epsilon - \mu\mathbf{j} \tag{36}$$

For the momentum flux (corresponding to the "momentum current density"), it is customary to introduce the so-called momentum flux tensor Π of rank 2, whose elements are given by

$$\Pi_{ij} = \int \frac{\mathrm{d}^d k}{(2\pi)^d}\, k_i v_j f \tag{37}$$

Lastly, it is convenient to define terms due to integrals over the external force term of the Boltzmann equation. To this end, the force density

$$\boldsymbol{\mathcal{F}}^{\text{ext}} = \int \frac{\mathrm{d}^d k}{(2\pi)^d}\, \mathbf{F}^{\text{ext}} f \tag{38}$$

is introduced, as well as a Joule heating term

$$h = \int \frac{\mathrm{d}^d k}{(2\pi)^d}\, \mathbf{v}\cdot\mathbf{F}^{\text{ext}} f \tag{39}$$

The choice of naming for this term becomes apparent when the external force is caused by an applied electric field $\mathbf{E}$. Then, if the particles have charge q, the Joule heating term becomes

$$h = \left(q\cdot\int \frac{\mathrm{d}^d k}{(2\pi)^d}\, \mathbf{v} f\right)\cdot\mathbf{E} = \mathbf{j}^{\text{el}}\cdot\mathbf{E} \tag{40}$$

where the right-hand side now describes the familiar rate at which heat is produced per unit volume by an electric current.

3.1 Equations of Fluid Dynamics

Many of the quantities defined above are related to one another via a set of three equations in an elegant way, by multiplying the Boltzmann equation by suitable functions and then integrating it over momentum. These equations will turn out to describe the conservation of particle number, momentum, and energy, respectively. This procedure also highlights the ties between the Boltzmann equation on the one hand, and the equations of fluid dynamics on the other. The discussion below again closely follows the treatment of Lifshitz and Pitaevskii [7].

To obtain the first equation, the Boltzmann equation (2) is written in index notation as

$$\frac{\partial f}{\partial t} + \sum_j v_j \frac{\partial f}{\partial r_j} + \sum_j F_j^{\text{ext}} \frac{\partial f}{\partial k_j} = \mathcal{C}[f] \tag{41}$$

Recalling that $\mathbf{v} = \frac{\partial \epsilon}{\partial \mathbf{k}}$ is independent of position, it follows that $\mathbf{v} \cdot \frac{\partial f}{\partial \mathbf{r}} = \nabla \cdot (\mathbf{v} f)$, which in index notation reads as

$$v_i \frac{\partial f}{\partial r_j} = \frac{\partial}{\partial r_j} (v_j f) \tag{42}$$

Similarly, assuming the external forces do not depend on momentum, the analogous relation

$$F_j^{\text{ext}} \frac{\partial f}{\partial k_j} = \frac{\partial}{\partial k_j} \left(F_j^{\text{ext}} f \right) \tag{43}$$

holds. The procedure is now to integrate (41) over momentum, which (incidentally) is the same as multiplying both sides by 1 and then integrating. This results in

$$\begin{aligned} \int \frac{\mathrm{d}^d k}{(2\pi)^d} \left(\frac{\partial f}{\partial t} + \sum_j \frac{\partial}{\partial r_j} (v_j f) + \sum_j \frac{\partial}{\partial k_j} \left(F_j^{\text{ext}} f \right) \right) &= \frac{\partial}{\partial t} \left(\frac{\mathrm{d}^d k}{(2\pi)^d} \, f \right) + \sum_j \frac{\partial}{\partial r_j} \left(\frac{\mathrm{d}^d k}{(2\pi)^d} \, v_j f \right) \\ &\quad + \sum_j \int \frac{\mathrm{d}^d k}{(2\pi)^d} \, \frac{\partial}{\partial k_j} \left(F_j^{\text{ext}} f \right) \\ &= \frac{\partial n}{\partial t} + \sum_j \frac{\partial j_j}{\partial r_j} + 0 \\ &= \frac{\partial n}{\partial t} + \nabla \cdot \mathbf{j} \end{aligned} \tag{44}$$

In the first line, the integral over the force term can be evaluated using the divergence theorem, resulting in a boundary term where $F_j^{\text{ext}} f$ is evaluated at infinite values of the momentum. Requiring that the distribution vanishes for infinite values of the kinematic variables therefore makes the integral vanish.

For the right-hand side of the Boltzmann equation, the integral over the collision integral must be required to vanish if the collision processes involved conserve particle number; this is shown in Appendix A. That is, conservation of particle number in collision processes ensures that

$$\int \frac{\mathrm{d}^d k}{(2\pi)^d} \, \mathcal{C}[f] = 0 \tag{45}$$

Therefore, the integrated Boltzmann equation reads

$$\frac{\partial n}{\partial t} + \nabla \cdot \mathbf{j} = 0 \tag{46}$$

which is the familiar continuity equation. In this way, the conservation of particle number in the microscopic sense, due to collisions conserving particle number, is reflected in one of the macroscopic equations for the system.

To obtain the second equation, (41) is first multiplied by a component of the momentum k_i, and then integrated over momentum. The multiplied equation takes the form

$$k_i \frac{\partial f}{\partial t} + \sum_j k_i \frac{\partial}{\partial r_j} (v_j f) + \sum_j k_i \frac{\partial}{\partial k_j} \left(F_j^{\text{ext}} f \right) = k_i \mathcal{C}[f] \tag{47}$$

The two first terms of the left-hand side can immediately be written as

$$k_i \frac{\partial f}{\partial t} = \frac{\partial}{\partial t}\left(k_i f\right) \tag{48a}$$

$$k_i \frac{\partial}{\partial r_j}\left(v_j f\right) = \frac{\partial}{\partial r_j}\left(k_i v_j f\right) \tag{48b}$$

As for the third term, the product rule gives

$$k_i \frac{\partial}{\partial k_j}\left(F_j^{\text{ext}} f\right) = \frac{\partial}{\partial k_j}\left(k_i F_j^{\text{ext}} f\right) - \delta_{ij} F_j^{\text{ext}} f \tag{49}$$

In particular, when the above expression is integrated over momentum, the first term above will give a vanishing contribution due to the divergence theorem, for the same reasons as in (44). Thus, the integral over the left-hand side of (47) yields

$$\begin{aligned}\int \frac{\mathrm{d}^d k}{(2\pi)^d}\left(k_i \frac{\partial f}{\partial t} + \sum_j k_i \frac{\partial}{\partial r_j}\left(v_j f\right) + \sum_j k_i \frac{\partial}{\partial k_j}\left(F_j^{\text{ext}} f\right)\right) &= \frac{\partial}{\partial t}\left(\int \frac{\mathrm{d}^d k}{(2\pi)^d}\, k_i f\right) + \sum_j \frac{\partial}{\partial r_j}\left(\int \frac{\mathrm{d}^d k}{(2\pi)^d}\, k_i v_j f\right) \\ &\quad + \sum_j \delta_{ij} \int \frac{\mathrm{d}^d k}{(2\pi)^d}\, F_j^{\text{ext}} f \\ &= \frac{\partial n_i^k}{\partial t} + \sum_j \frac{\partial \Pi_{ij}}{\partial r_j} - \sum_j \delta_{ij} \mathcal{F}_j^{\text{ext}} \\ &= \frac{\partial n_i^k}{\partial t} + \sum_j \frac{\partial \Pi_{ij}}{\partial r_j} - \mathcal{F}_i^{\text{ext}}\end{aligned} \tag{50}$$

On the other hand, if momentum is conserved in collision processes, then

$$\int \frac{\mathrm{d}^d k}{(2\pi)^d}\, \mathbf{k}\mathcal{C}[f] = \mathbf{0} \tag{51}$$

which is again shown in Appendix A. Therefore, the second relation reads

$$\frac{\partial n_i^k}{\partial t} + \sum_j \frac{\partial \Pi_{ij}}{\partial r_j} - \mathcal{F}_i^{\text{ext}} = 0 \tag{52}$$

This equation expresses conservation of momentum in the absence of external forces [7], again in the functional form of a continuity equation; the momentum density is related to the "momentum current density", which is the momentum flux tensor.

Finally, to obtain the third relation, (41) is multiplied by the dispersion ϵ and then integrated. Following similar steps as above, it is found that

$$\frac{\partial n^\epsilon}{\partial t} + \nabla \cdot \mathbf{j}^\epsilon - h = 0 \tag{53}$$

where

$$\int \frac{\mathrm{d}^d k}{(2\pi)^d}\, \epsilon \mathcal{C}[f] = 0 \tag{54}$$

provided energy is conserved in collisions, which also discussed in Appendix A. Much like the previous relations, (53) expresses another conservation law as a continuity equation; this time, energy is conserved in the system in the absence of external forces, by relating the energy density to the energy current.

Together, equations (46), (52) and (53) provide a set of fluid dynamics equations, with each expressing a form of conservation law. Strictly speaking, these equations need to be fully related to macroscopic fields to rightfully be called fluid dynamics, but this is beyond the scope of this thesis (the interested reader is referred to [7] for a discussion on this). To thus observe hydrodynamic behaviour in electronic systems, it is crucial that the collision processes involved conserve particle number, momentum, and energy. At the very least, such processes ought to dominate the system, so that conservation-violating processes are negligible [9].

3.2 Transport Coefficients and the Onsager Reciprocal Relations

The *Onsager reciprocal relations* are a set of equations relating *transport coefficients* in a system described by irreversible processes. Below, these relations will be presented without proof, referring to [14] for a formal derivation.

In the most general case, it is assumed there are *generalised currents* $\mathbf{j}_n, \mathbf{j}_2, \ldots, \mathbf{j}_n$, being influenced by *generalised forces* $\mathbf{X}_1, \ldots, \mathbf{X}_n$. These currents can then be expressed as linear functions of the forces [15]:

$$\mathbf{j}_i = \sum_j L_{ij} \mathbf{X}_j \tag{55}$$

with L_{ij} the transport coefficients. Generally, the transport coefficients are matrices, but given sufficient symmetry in the system they reduce to multiples of the identity matrix, so that they may effectively be treated as real numbers.

Next, one defines the generalised currents and forces more specifically by relating them pairwise such that the rate of entropy density production s in the system is given by

$$\frac{\partial s}{\partial t} = \sum_i \mathbf{j}_i \cdot \mathbf{X}_i \tag{56}$$

Then, the Onsager reciprocal relations state that

$$L_{ij} = L_{ji} \tag{57}$$

In other words, the matrix of transport coefficients is symmetric. This formulation of the relations is valid when no magnetic field is present, or generally when the system and all the forces exhibit time-reversal symmetry.

The Onsager relations, in practice, reduce the number of transport coefficients that need to be computed to fully describe the transport phenomena of the system. In particular, the *thermoelectric* transport due to an external electric field $\mathbf{E}$ together with a temperature gradient ∇T will be investigated below, in preparation for the calculations in Sections 5 and 6. In the case of only an external electric field, the rate of entropy density production due to Joule heating is given by

$$\frac{\partial s}{\partial t} = \frac{\mathbf{j}^{\text{el}} \cdot \mathbf{E}}{T} \tag{58}$$

where $\mathbf{j}^{\text{el}}$ is the electric current density in the system. Instead, in the presence of only a thermal gradient, a heat current $\mathbf{j}^q$ would give rise to entropy production at a rate [15]

$$\frac{\partial s}{\partial t} = \nabla \cdot \left(\frac{\mathbf{j}^q}{T} \right) \tag{59}$$

In particular, if the heat current is constant, as is often the case in an experimental setting, it can be taken outside the derivative to give

$$\begin{aligned} \frac{\partial s}{\partial t} &= \mathbf{j}^q \cdot \nabla \left(\frac{1}{T} \right) \\ &= -\mathbf{j}^q \cdot \frac{\nabla T}{T^2} \end{aligned} \tag{60}$$

which allows for the casting of this equation in the canonical form (56). To this end, the rate of entropy production in the presence of both an electric field and a thermal gradient is

$$\frac{\partial s}{\partial t} = \mathbf{j}^{\text{el}} \cdot \frac{\mathbf{E}}{T} - \mathbf{j}^q \cdot \frac{\nabla T}{T^2} \tag{61}$$

Moreover, the generalised currents are set equal to the electric and heat currents, respectively. That is, $\mathbf{j}_1$ is set to be the electric current $\mathbf{j}^{\text{el}}$, and $\mathbf{j}_2$ the heat current $\mathbf{j}^q$. It follows from this choice that the generalised forces are

$$\mathbf{X}_1 = \frac{\mathbf{E}}{T} \tag{62a}$$

$$\mathbf{X}_2 = -\frac{\nabla T}{T^2} \tag{62b}$$

Then, the currents are expressed in terms of the forces via (55) as

$$\mathbf{j}^{\text{el}} = \frac{L_{11}}{T}\mathbf{E} - \frac{L_{12}}{T^2}\nabla T \tag{63a}$$

$$\mathbf{j}^q = \frac{L_{21}}{T}\mathbf{E} - \frac{L_{22}}{T^2}\nabla T \tag{63b}$$

and the Onsager relation (57) implies that $L_{21} = L_{12}$. It is helpful to relate the coefficients L_{ij} to more familiar quantities. Firstly, the *electrical conductivity* σ is defined by the relation

$$\mathbf{j}^{\text{el}} = \sigma \mathbf{E} \tag{64}$$

in the absence of a thermal gradient. Thus,

$$\sigma = \frac{L_{11}}{T} \tag{65}$$

is immediately read off from (63). Next, it is convenient to introduce the shorthand notation

$$\alpha = \frac{L_{12}}{T^2} \tag{66}$$

which is related to the *thermopower* Q, also called the *Seebeck coefficient*, via

$$\alpha = \frac{Q\sigma}{T} \tag{67}$$

Thus, α captures how a temperature gradient in turn induces an electrical field inside a material. Then, the Onsager relation yields

$$\frac{L_{21}}{T} = T\alpha \tag{68}$$

Moreover, the shorthand symbol

$$\overline{\kappa} = \frac{L_{22}}{T^2} \tag{69}$$

is defined for convenience. Finally, the *thermal conductivity* κ is defined by

$$\mathbf{j}^q = -\kappa \nabla T \tag{70}$$

in the absence of an electric current, $\mathbf{j}^{\text{el}} = \mathbf{0}$. The requirement of a vanishing electric current forces $\mathbf{0} = \sigma\mathbf{E} - \alpha\nabla T$, or

$$\mathbf{E} = \frac{\alpha}{\sigma}\nabla T \tag{71}$$

Inserting this into the relation for the heat current,

$$\begin{aligned} \mathbf{j}^q &= T\alpha\mathbf{E} - \overline{\kappa}\nabla T \\ &= \left(\frac{T\alpha^2}{\sigma} - \overline{\kappa}\right)\nabla T \end{aligned} \tag{72}$$

The thermal conductivity is therefore expressed as

$$\kappa = \overline{\kappa} - \frac{T\alpha^2}{\sigma} \tag{73}$$

The interpretation of this relation is that, to ensure a vanishing electrical current, an electric field is set up in the material, reducing the heat current in turn. This makes it so that κ is reduced from $\overline{\kappa}$ by the amount $\frac{T\alpha^2}{\sigma}$.

Put together, the relations of the electric and heat currents in the system to the electric field and the thermal gradient can be summarised in matrix notation as

$$\begin{pmatrix} \mathbf{j}^{\text{el}} \\ \mathbf{j}^q \end{pmatrix} = \begin{pmatrix} \sigma & \alpha \\ T\alpha & \overline{\kappa} \end{pmatrix} \begin{pmatrix} \mathbf{E} \\ -\nabla T \end{pmatrix} \tag{74}$$

4 Dirac Materials

Over the past few decades, so-called *Dirac materials* have gained widespread interest due to the universal properties found in different materials belonging to the class. Examples of Dirac materials include superfluids such as ^{3}He, graphene, topological insulators, and Weyl semimetals [16]. Despite the seemingly drastic differences of these materials, they are united by a common feature, which indeed is also the formal definition of Dirac matter. Namely, Dirac materials possess a quasiparticle description whose low-energy spectrum is governed by a Dirac-like equation [17], as opposed to the usual Schrödinger equation. For two-dimensional Dirac materials, the corresponding Dirac hamiltonian H_D assumes the form

$$H_D(\mathbf{k}) = v_F\boldsymbol{\sigma}\cdot\mathbf{k} + mv_F^2\sigma_z \tag{75}$$

with $\boldsymbol{\sigma} = (\sigma^x, \sigma^y)$ and σ^z the Pauli matrices, and where v_F is the Fermi velocity of the quasiparticles and m their effective mass. Particles described by such a hamiltonian could be called "Dirac particles". This is in contrast to e.g. the conventional understanding of metals, where low-energy excitations are accurately described by a free-particle Schrödinger hamiltonian H_S of the form

$$H_S(\mathbf{k}) = \frac{\mathbf{k}^2}{2m^*} \tag{76}$$

with m^* the effective mass of the particles. Particles instead described by this hamiltonian might be called "Schrödinger particles".

The hamiltonian (75) describes a two-band system with an energy gap $\Delta = mv_F^2$. In the limit of a vanishing gap, corresponding to $m \to 0$, the quasiparticles thus become massless, and the dispersion becomes linear in $k = |\mathbf{k}|$, unlike the parabolic dispersion of conventional metals. This is portrayed in Figure 2, displaying the typical *Dirac cones* associated with Dirac meterials, as well as the *Dirac points* where the two bands touch. However, even for systems with non-zero mass m the Dirac particles described are qualitatively different from Schrödinger particles, for a few reasons [18]; in a Dirac material, the particles and holes have the same effective mass m, and this mass is also intimately related to the band gap Δ. In conventional metals, there is no generic reason to expect either condition to be met.

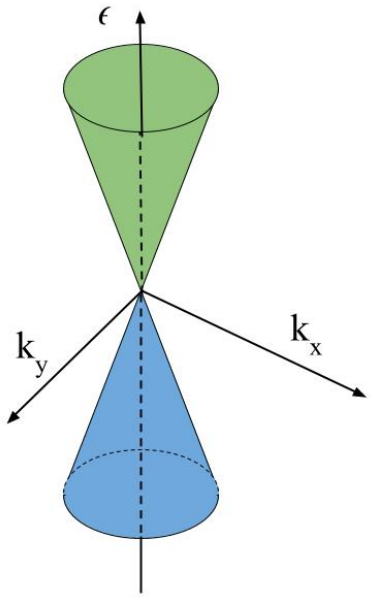

Figure 2: Band structure of a two-dimensional Dirac material, describing massless particles.

For Dirac materials in three dimensions, all three Pauli matrices are used in the term proportional to $\boldsymbol{\sigma} \cdot \mathbf{k}$ of the Dirac hamiltonian. In other words, a three-dimensional Dirac material necessarily describes massless Dirac particles with hamiltonian

$$H_D(\mathbf{k}) = v_F \boldsymbol{\sigma} \cdot \mathbf{k} \tag{77}$$

where, this time, $\boldsymbol{\sigma} = (\sigma^x, \sigma^y, \sigma^z)$. Since this hamiltonian precisely reproduces the Weyl equation of particle physics, three-dimensional Dirac materials are known as Weyl semimetals. One-dimensional Dirac materials have also very recently been observed [19], in the form of silicon nanoribbons.

Due to the fact that Dirac particles are described by a Dirac-like equation, or equivalently that their dispersion is linear in momentum, these systems exhibit many of the properties typically only seen for relativistic particles; indeed, Dirac particles are often called "relativistic" [9] since the governing equations are functionally the same. It is important, however, to recall that Dirac quasiparticles do not fully resemble truly relativistic particles. For instance, since Coulomb interactions propagate at the speed of light $c \gg v_F$, they are effectively instantaneous in a Dirac material. Nonetheless, some features carry over, as described below.

A first sign of relativistic phenomena in Dirac matter stems from the presence of the Pauli matrices in the Dirac hamiltonian, indicating that Dirac particles all share a quantity resembling spin. This quantity is called *pseudospin*, and is typically unrelated to the spins of the real constituent particles that make up the Dirac material. Instead, the pseduospin usually arises from some symmetry property of the Dirac material. For graphene, as will be discussed in Section 4.1, the cause is sublattice symmetry.

More explicitly, a measure of whether any particle behaves relativistically or not is given by the ratio of its kinetic energy to its rest mass, i.e. $\frac{kc}{mc^2}$. In the ultra-relativistic limit of $kc \gg mc^2$, the so-called *chirality* Λ is conserved, given by

$$\Lambda = \frac{\boldsymbol{\sigma} \cdot \mathbf{k}}{|\mathbf{k}|} \tag{78}$$

and taking values ± 1. Thus, chirality distinguishes between particles that have spin and momentum aligned or anti-aligned, respectively. In Dirac materials, the spin $\boldsymbol{\sigma}$ is replaced by the pseudospin, but the resulting chirality is still conserved in the ultrarelativistic regime. In fact, gapless Dirac materials also allow for the exact conservation of chirality, since these systems correspond to taking the vanishing mass limit $m \to 0$.

The conservation of chirality has immediate consequences for transport in Dirac materials. To ensure conservation, back scattering of particles $\mathbf{k} \to -\mathbf{k}$ must be accompanied by pseudospin flips $\boldsymbol{\sigma} \to -\boldsymbol{\sigma}$. It can be shown that back scattering amplitudes given by such processes are greatly suppressed in Dirac materials [20]. Thus, back scattering of Dirac particles due to e.g. an impurity potential that conserves chirality is forbidden. This is a manifestation of the so-called Klein paradox [5], where ultrarelativistic particles are able to tunnel through potential barriers of arbitrary width and height.

Another effect of relativistic nature is the so-called Zitterbewegung, or "jittery motion", usually associated with relativistic particles. For massless relativistic (and "relativistic") particles, their momenta and energies differ only by a factor of $\hbar v_F$. Therefore, the Heisenberg uncertainty relations couple for positions and momenta on the one hand, and times and energies no the other. This is in contrast to ordinary quantum particles, where the two relations are independent. Zitterbewegung has the rather drastic implication that an intially particle-like state may include hole-like states as the state evolves [21].

There are a host of other properties that are universally observed in Dirac materials, intimately connected to the shared low-energy spectrum and thus independent of the nature of specific Dirac materials. As an example, the density of states close to a Dirac point goes as

$$N_0(E) \sim E^{d-1} \tag{79}$$

with d the dimension of the system [16]. Therefore, Dirac materials have response functions characterised by a set of exponents, i.e. power-law behaviour. For instance, while the specific heat C goes

as

$$C(T) \sim T \tag{80}$$

at low temperatures in ordinary metals, the corresponding power-law behaviour in Dirac materials is

$$C(T) \sim T^d \tag{81}$$

which has been observed e.g. in cuprate superconductors [22].

4.1 Graphene

Graphene is perhaps the most famous Dirac material, and also the first experimental discovery of a two-dimensional crystal [6]. It consists of carbon atoms arranged in a honeycomb lattice, schematically depicted in Figure 3. The reason for this structure is the fact that carbon atoms have four valence electrons, three of which hybridise into sp^2 orbitals which happen to lie in a plane at 120° angles to one another. Thus, each carbon atom provides one electron to the lattice as a conduction electron, and it follows that undoped graphene is half-filled and charge neutral.

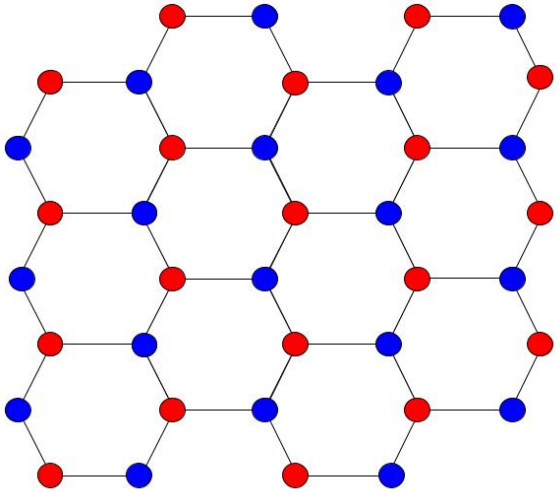

Figure 3: The two-dimensional lattice structure of graphene, with blue and red colours both indicating carbon atoms. Here, the colours represent a sublattice partition.

The discovery of graphene came as a surprise to the scientific community [23], because although graphene had been investigated theoretically for over sixty years before its discovery [24, 25] (then considered a "single layer of graphite"), it was long conjectured that two-dimensional crystals were unstable and could never physically be realised [26]. In fact, the argument for this dates back to the 1930's [27], and was later formalised in the famous Mermin-Wagner theorem [28]. In essence, the physical argument is that thermal fluctuations at finite temperatures grow so large, in dimensions strictly less than 3, that atoms are displaced on the order of the interatomic distance of the lattice, thereby destroying the crystalline structure of the sample. In spite of this, graphene was indeed created experimentally, and found to be both stable and highly symmetric [6]. This fact can be

reconciled with theory by noting that graphene has strong interatomic bonds suppressing thermal fluctuations, together with the observation that graphene does "ripple" in the out-of-plane direction ever so slightly [29, 30].

Given the structure of the atomic orbitals of graphene, it is well-described by a tight-binding model with nearest-neighbour hopping. With $t \approx 2.8$ eV [21] the so-called hopping parameter, the tight-binding hamiltonian can be written in first quantisation as

$$H = -t \sum_{\langle ij \rangle} c_i^\dagger c_j + c_j^\dagger c_i \tag{82}$$

with $c_i^\dagger, c_i$ the electronic creation and annihilation operators at lattice site i, respectively, and where the sum runs over nearest neighbours i, j not including $i = j$. These obey the usual fermionic commutation relations:

$$\{c_i, c_j\} = 0 \tag{83a}$$

$$\left\{c_i, c_j^\dagger\right\} = \delta_{ij} \tag{83b}$$

$$\left\{c_i^\dagger, c_j^\dagger\right\} = 0 \tag{83c}$$

The hamiltonian description (82) ignores a few interactions worthy of mention. Firstly, electronic spin is ignored, and this is justifiable since the strength of spin-orbit coupling in graphene is negligible compared to the other interactions present [31, 32]. Secondly, Coulomb interactions are neglected. These will be taken into account by suitable modifications to the collision integral in Sections 5 and 6. Impurities will also be considered in that section. Nonetheless, (82) captures the essential aspects of graphene, as shown below.

Because of its hexagonal nature, the honeycomb lattice is not fundamental, i.e. it is not a Bravais lattice. To remedy this, two sublattices are defined, as indicated by the colour scheme in Figure 3. For instance, the red sublattice could be labelled by "A" and the blue by "B". Then, by choosing a unit cell that encloses one atom from each sublattice, the resulting lattice is triangular, and therefore Bravais. One choice of unit cell is shown in Figure 4.

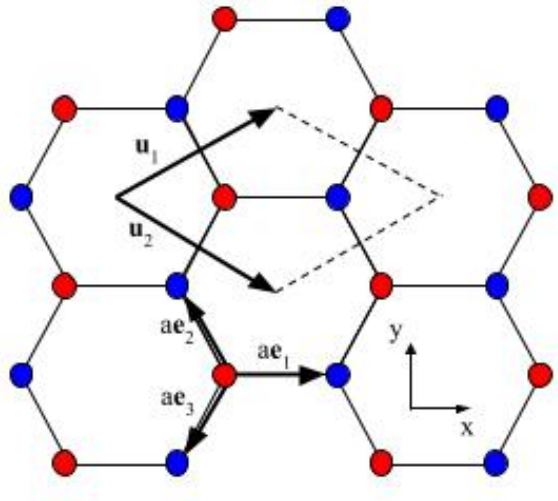

Figure 4: The vectors $\mathbf{u}_1, \mathbf{u}_2$ together with the dashed lines provide one choice of a Bravais unit cell for graphene. Also included are the displacement vectors $\mathbf{e}_1, \mathbf{e}_2, \mathbf{e}_3$, as well as a choice of coordinate system.

Moreover, it is evident that electrons can only hop between atoms of different sublattices. The displacements of electrons due to this hopping is given by $\pm a\mathbf{e}_1$, $\pm\mathbf{e}_2$ or $\pm\mathbf{e}_3$, with $a \approx 0.14$ nm the interatomic spacing and where

$$\mathbf{e}_1 = \hat{\mathbf{x}} \tag{84a}$$

$$\mathbf{e}_2 = -\frac{1}{2}\hat{\mathbf{x}} + \frac{\sqrt{3}}{2}\hat{\mathbf{y}} \tag{84b}$$

$$\mathbf{e}_2 = -\frac{1}{2}\hat{\mathbf{x}} - \frac{\sqrt{3}}{2}\hat{\mathbf{y}} \tag{84c}$$

in terms of the coordinate system chosen in Figure 4. The basis vectors of the Bravais lattice are then related to the above vectors as

$$\mathbf{u}_1 = a\left(\mathbf{e}_1 - \mathbf{e}_3\right) \tag{85a}$$

$$\mathbf{u}_2 = a\left(\mathbf{e}_1 - \mathbf{e}_2\right) \tag{85b}$$

It follows that the reciprocal lattice has a basis $\mathbf{G}_1, \mathbf{G}_2$ defined by $\mathbf{G}_i \cdot \mathbf{u}_j = 2\pi\delta_{ij}$, and is again triangular. This, in turn, implies that the reciprocal lattice of the (original) honeycomb lattice is again a honeycomb lattice, and in particular that the first Brillouin zone is a regular hexagon. This is schematically depicted in Figure 6.

Given the partition of the carbon atoms into two sublattices, it is helpful to define creation and annihilation operators on each sublattice. To this end, $a_i^\dagger, a_i$ are defined as the creation and annihilation operators, respectively, on lattice site i of sublattice A. Similarly, $b_i^\dagger, b_i$ are defined on sublattice B. Their respective commutation relations are then derived from equations (84) in a srtaightforward manner. In this way, the hamiltonian (82) can be written as

$$H = -t\sum_{\langle ij\rangle} a_i^\dagger b_j + b_j^\dagger a_i \tag{86}$$

To find the spectrum of the above hamiltonian, the operators are first Fourier transformed. Specifically, the Fourier transforms of a_i, b_i, denoted $\alpha_{\mathbf{k}}, \beta_{\mathbf{k}}$ respectively, are defined by

$$a_{\mathbf{r}_i} = \sqrt{\frac{2}{N}} \sum_{\mathbf{k}\in 1\text{B.Z}} e^{-i\mathbf{k}\cdot\mathbf{r}_i}\alpha_{\mathbf{k}} \tag{87a}$$

$$b_{\mathbf{r}_i+a\mathbf{e}_1} = \sqrt{\frac{2}{N}} \sum_{\mathbf{k}\in 1\text{B.Z}} e^{-i\mathbf{k}\cdot(\mathbf{r}_i+a\mathbf{e}_1)}\beta_{\mathbf{k}} \tag{87b}$$

with the creation operators $\alpha^\dagger_{\mathbf{k}}, \beta^\dagger_{\mathbf{k}}$ obtained by hermitian conjugation. Here, $\mathbf{r}_i$ denotes the position of the i'th atom in sublattice A, so that $\mathbf{r}_i + a\mathbf{e}_1$ describes the position of the atom from sublattice B contained within the same unit cell. Also, the notation above indicates that the sums over momenta are to be taken over the first Brillouin zone, and N denotes the total number of lattice sites in the system.

After Fourier transforming the hamiltonian, assuming periodic boundary conditions, the result is easiest written in matrix notation as

$$\begin{aligned} H &= -t \sum_{\mathbf{k}\in 1\text{B.Z.}} \begin{pmatrix} \alpha^\dagger_{\mathbf{k}} & \beta^\dagger_{\mathbf{k}} \end{pmatrix} \begin{pmatrix} 0 & e^{-ia\mathbf{k}\cdot\mathbf{e}_1} + e^{-ia\mathbf{k}\cdot\mathbf{e}_2} + e^{-ia\mathbf{k}\cdot\mathbf{e}_3} \\ e^{ia\mathbf{k}\cdot\mathbf{e}_1} + e^{ia\mathbf{k}\cdot\mathbf{e}_2} + e^{ia\mathbf{k}\cdot\mathbf{e}_3} & 0 \end{pmatrix} \begin{pmatrix} \alpha_{\mathbf{k}} \\ \beta_{\mathbf{k}} \end{pmatrix} \\ &:= \sum_{\mathbf{k}\in 1\text{B.Z.}} \begin{pmatrix} \alpha^\dagger_{\mathbf{k}} & \beta^\dagger_{\mathbf{k}} \end{pmatrix} H(\mathbf{k}) \begin{pmatrix} \alpha_{\mathbf{k}} \\ \beta_{\mathbf{k}} \end{pmatrix} \end{aligned} \tag{88}$$

It follows that the dispersion is given by

$$\begin{aligned} \epsilon(\mathbf{k}) &= \pm\sqrt{\det\left(H(\mathbf{k})\right)} \\ &= \pm t \left| e^{-ia\mathbf{k}\cdot\mathbf{e}_1} + e^{-ia\mathbf{k}\cdot\mathbf{e}_2} + e^{-ia\mathbf{k}\cdot\mathbf{e}_3} \right| \end{aligned} \tag{89}$$

which shows that the quasiparticles in graphene are particle-hole symmetric. This band structure is plotted in Figure 5. In particular, the two bands touch at two inequivalent points $\mathbf{K}, \mathbf{K}'$ (i.e. points not related by reciprocal lattice vectors) on the boundary of the first Brillouin zone, which is to say that $\epsilon(\mathbf{K}) = \epsilon(\mathbf{K}') = 0$. A possible choice is

$$\mathbf{K} = \frac{4\pi}{3\sqrt{3}a}\left(\frac{\sqrt{3}}{2}\hat{\mathbf{x}} + \frac{1}{2}\hat{\mathbf{y}}\right) \tag{90a}$$

$$\mathbf{K}' = -\frac{4\pi}{3\sqrt{3}a}\left(\frac{\sqrt{3}}{2}\hat{\mathbf{x}} + \frac{1}{2}\hat{\mathbf{y}}\right) = -\mathbf{K} \tag{90b}$$

and these points are also indicated in Figure 6. The vanishing of the dispersion at two points implies that graphene has two Dirac points, and also indicates that the quasiparticles are massless, due to the absence of an energy gap. Thus, in a low-energy description it is as if the electrons and holes "lose" their mass in graphene, and for this reason the quasiparticles in graphene will continue to be referred to as electrons and holes.

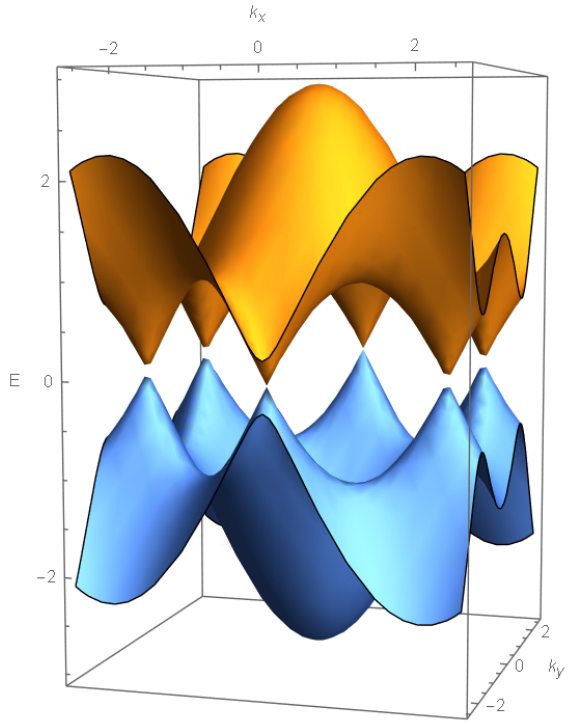

Figure 5: The band structure of graphene, with the electron band in yellow and the hole band in blue. Here the wavenumbers, k_x, k_y are displayed in units of a^{-1} and the energy E in units of t. (In the plot it may appear some Dirac points are gapped; this is not the case, but is rather due to the inaccuracy of the plotting program.)

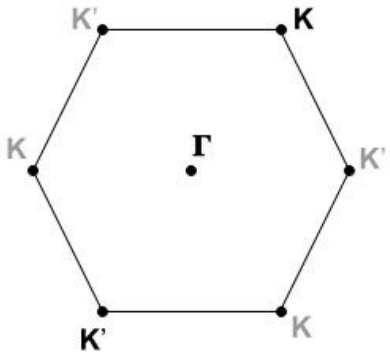

Figure 6: The first Brillouin zone of graphene, with $\mathbf{\Gamma}$ its center and $\mathbf{K}, \mathbf{K}'$ its two (inequivalent) Dirac points. Indicated in gray text is also how the remaining corners of the Brillouin zone are related to $\mathbf{K}, \mathbf{K}'$ via reciprocal lattice vectors.

Moreover, expanding the dispersion in powers of $|\mathbf{k}|$ for small $\mathbf{k}$, it is found that

$$\epsilon(\mathbf{K}+\mathbf{k}) \approx \pm\frac{3at}{2}|\mathbf{k}| \tag{91a}$$

$$\epsilon(\mathbf{K}'+\mathbf{k}) \approx \pm\frac{3at}{2}|\mathbf{k}| \tag{91b}$$

This is precisely the signature "relativistic" dispersion of a Dirac material, and from the relation

$$\epsilon(\mathbf{k}) \approx v_F|\mathbf{k}| \tag{92}$$

the Fermi velocity v_F of graphene can be read off as

$$v_F = \frac{3at}{2\hbar} \approx 1.1 \cdot 10^6 \text{ m/s} \tag{93}$$

where the factor of $\hbar$ has been restored from dimensional analysis. Finally, to make the connection to Dirac materials fully explicit, it remains to cast the hamiltonian in the form (75). For this, it can be seen that near either Dirac point, $H(\mathbf{k})$ goes as

$$H(\mathbf{K}+\mathbf{k}) \approx v_F \begin{pmatrix} 0 & k_x - ik_y \\ k_x + ik_y & 0 \end{pmatrix} = v_F \boldsymbol{\sigma}\cdot\mathbf{k} \tag{94a}$$

$$H(\mathbf{K}'+\mathbf{k}) \approx -v_F \begin{pmatrix} 0 & k_x - ik_y \\ k_x + ik_y & 0 \end{pmatrix} = -v_F \boldsymbol{\sigma}\cdot\mathbf{k} \tag{94b}$$

up to an overall phase factor, which can be absorbed either into the definitions of the creation and annihilation operators or the wavefunction itself. The opposite signs in the relations above also show that the sign of the particle chirality depends on which Dirac point the particle is near; around $\mathbf{K}$ electrons have a chirality of +1 and holes that of -1, and at $\mathbf{K}'$ the signs are flipped.

Since the Dirac points themselves formally constitute a degree of freedom of the particles, in the same way the spin of a particle normally does, this is usually referred to as the *valley* degree of freedom. It is this also this degree that assumes the role of pseudospin for graphene. From here onwards, it will be assumed that all particles have the same pseudospin for simplicity. This is a fair assumption since the momentum transfer $q_{\mathbf{K}\leftrightarrow\mathbf{K}'}$ needed to scatter a particle from one valley to the other is large

$$q_{\mathbf{K}\leftrightarrow\mathbf{K}'} \approx |\mathbf{K}-\mathbf{K}'| = \frac{8\pi}{3\sqrt{3}a} \approx 4 \cdot 10^{10} \text{ m}^{-1} \tag{95}$$

and can safely be neglected in a low-energy theory. Thus, the 2 states from the valley degree of freedom, together with the 2 spin states of the real spins of the electrons, this theory describes $\mathcal{N} = 4$ flavours of particles, of which only one will be considered at a time.

While ideal graphene indeed possesses a gapless dispersion, there are multiple ways to introduce a gap, all of which related to breaking its sublattice symmetry. For instance, spin-orbit coupling will create a gap [33], as will straining graphene [34]. Moreover, the formation of so-called charge puddles may locally spoil the particle-hole symmetry of graphene. These occur when charged impurities, either in the graphene sheet [35] or in a substrate on which it is placed [36], give rise to local deviations in the chemical potential. Near the charge neutrality point, such impurities thus give rise to local regions of excess positive or negative charge, referred to as charge puddles.

4.1.1 Electron Hydrodynamics and Graphene

A few qualities of graphene make it an excellent candidate to observe electron hydrodynamics in. Naturally, all the universal properties of Dirac materials listed above could be restated here, but there are also a few points specific to graphene which make it especially attractive. One is the development of the process of fabricating graphene, to the point where so-called ultraclean samples can be obtained [37, 38]. This ensures that electron-electron interactions dominate over impurity effects, implying the conservation laws (46), (52), and (53) are very nearly met. Thus, the characteristic properties of electron hydrodynamics, as opposed to behaviour due to impurity-dominated scattering, can and have been observed in graphene; for instance, the flow profile of Poiseuille flow was recently directly observed [39], while another experiment confirmed the presence of whirlpools in electronic flow [40].

From a more practical standpoint, graphene also possesses a relatively simple band structure, as seen in (89). This makes for easier calculations, and subsequently comparisons with experiments can be done more readily.

Moreover, tying in to the first point, graphene has relatively strong electron-electron interactions. This is best seen by introducing a "fine structure constant" α, in analogy with its counterpart $\alpha_{QED} \approx \frac{1}{137}$ from quantum electrodynamics. The dimensionless number α measures the ratio of the typical potential energy of an electron to its kinetic energy. On the one hand, the potential energy goes as $\frac{e^2}{4\pi\varepsilon r}$ with r the typical distance between electrons and ε the permittivity of graphene (not to be confused with the dispersion ϵ). On the other, the kinetic energy goes as $\hbar v_F q$, with q the average wavenumber of an electron. To within an order of magnitude, q can be taken as $1/r$, the inverse typical distance. Then,

$$\alpha = \frac{\frac{e^2}{4\pi\varepsilon r}}{\frac{\hbar v_F}{r}} = \frac{e^2}{4\pi\varepsilon\hbar v_F} \tag{96}$$

For a more direct comparison with α_{QED}, the above expression can be re-written slightly. With the known values of $v_F \approx 1.1 \cdot 10^6$ m/s and $1 \lesssim \varepsilon/\varepsilon_0 \lesssim 5$ [41] with ε_0 the vacuum permittivity, it follows that

$$\alpha = \frac{e^2}{4\pi\varepsilon_0\hbar c} \cdot \frac{c}{v_F} \cdot \frac{\varepsilon_0}{\varepsilon} = \alpha_{QED} \cdot \frac{c}{v_F} \cdot \frac{\varepsilon_0}{\varepsilon} \approx 1 \tag{97}$$

In other words, the relative strength of electron-electron interactions in graphene to that of quantum electrodynamics is about two orders of magnitude. This has drastic consequences for the thermalisation rate of the electron fluid, leading to a situation where the electron fluid appears to be in local equilibrium on all time scales which can be investigated experimentally [9, 42]. This validates the use of an expansion around local equilibrium in Sections 5 and 6.

Finally, graphene can easily be tuned to its *charge neutrality point* by setting the chemical potential to $\mu = 0$. In other words, the Fermi energy is placed such that it precisely crosses through the Dirac points of the bands, effectively reducing the Fermi surface down to a set of discrete (0-dimensional) points. This ensures a Dirac hamiltonian description is valid, with non-negligible densities of both electrons and holes. There are also remarkable predictions done for the charge neutrality point, including a finite electrical conductivity even in the clean limit [43, 44]; this is known as the *minimal conductivity problem*. However, it remains difficult experimentally to distinguish the "clean" electrical conductivity from other contributions such as disorder [9].

4.1.2 Phonons

While electrons and holes alone account for some of the transport phenomena in graphene, phonons are also needed to better model the system. On a fundamental level, phonons are a collective mode

available to any lattice system, and it is reasonable to include them in the study of such systems. However, to see the more specific need for their inclusion in the study of graphene, it is instructive to consider the impact of phonons on the transport coefficients of (74). Being neutrally charged, phonons are expected to have little impact on the electrical conductivity. On the other hand, phonons may very well have an impact on the heat conductivity through both electron-phonon scattering as well as phonon-phonon scattering. Indeed, even though electron-phonon interactions are weak in graphene in comparison to electron-electron interactions [42], electron-electron interactions only account for about 1% of the thermal conductivity κ in room-temperature graphene [9, 45].

Moreover, by incorporating phonons into the model, momentum conservation is ensured in the absence of disorder. That is, without the inclusion of phonons, electrons and holes may "lose" momentum to the phonon fluid in ways that are difficult to capture. Accounting for phonons thus ensures total momentum is conserved in clean systems, while momentum in the individual sectors (electrons, holes, phonons) may not be.

The phonon dispersion of graphene is most readily derived by considering graphite, and then restricting the resulting waves to a single layer. Over a series of papers [46, 47], the phonons in graphite were found to split into three nearly independent modes

$$\epsilon_b^1 = \left(v_t^2 \left(k_x^2 + k_y^2\right) + \frac{\zeta}{\pi^2 c^2} \sin^2\left(\pi c k_z\right) \right)^{1/2} \tag{98a}$$

$$\epsilon_b^2 = \left(v_l^2 \left(k_x^2 + k_y^2\right) + \frac{\zeta}{\pi^2 c^2} \sin^2\left(\pi c k_z\right) \right)^{1/2} \tag{98b}$$

$$\epsilon_b^3 = \left(4\pi^2\theta^2 \left(k_x^2 + k_y^2\right)^2 + \zeta \left(k_x^2 + k_y^2\right) + \frac{M^2}{\pi^2} \sin\left(\pi c k_z\right) \right)^{1/2} \tag{98c}$$

with $v_t, v_l, \zeta, \theta, M$ all constants related to the bulk properties of graphite, and where c is the inter-layer spacing. The above modes correspond to in-plane transverse waves, in-plane longitudinal waves, and out-of-plane waves, respectively. For a single layer, one sets $k_z = 0$ which yields

$$\epsilon_b^1 = v_t \sqrt{k_x^2 + k_y^2} = v_t |\mathbf{k}| \tag{99a}$$

$$\epsilon_b^2 = v_l \sqrt{k_x^2 + k_y^2} = v_l |\mathbf{k}| \tag{99b}$$

$$\epsilon_b^3 = \sqrt{4\pi^2\theta^2 \left(k_x^2 + k_y^2\right)^2 + \zeta \left(k_x^2 + k_y^2\right)} = \sqrt{4\pi^2\theta^2 |\mathbf{k}|^2 + \zeta |\mathbf{k}|} \tag{99c}$$

In particular, all three phonon modes are isotropic in $\mathbf{k}$, i.e. the dispersions are functions of $|\mathbf{k}|$ alone.

In Section 5, the model will be first be developed without phonons, and the resulting transport coefficients will be analysed. Then, phonons are incorporated in Section 6, and the same analysis is performed to compare the transport coefficients of the two models.

5 Electron-Hole Description

5.1 Model

For the initial model of graphene using the Boltzmann equation formalism, only electrons and holes are considered. Here, quantities related to electrons are indicated by a + index, and those of holes by a −. These signs are chosen such that

$$\epsilon_\pm(\mathbf{k}) = \pm v_F |\mathbf{k}| \tag{100}$$

gives the appropriate sign for the dispersions of the respective particle types. Thus, for instance, f_+ refers to the electron distribution, while $\mathbf{v}_- = \frac{\partial \epsilon_-}{\partial \mathbf{k}}$ denotes the velocity of a hole with momentum $\mathbf{k}$. Moreover, for notational convenience the expressions for derivatives are shortened, so that e.g. $\partial_t f_+ = \frac{\partial f_+}{\partial t}$ and $\partial_{\mathbf{k}} f_- = \frac{\partial f_-}{\partial \mathbf{k}}$.

In general, the two coupled Boltzmann equations describing an electron-hole system assume the form

$$\partial_t f_+ + \mathbf{v}_+ \cdot \partial_{\mathbf{r}} f_+ + \mathbf{F}_+^{\text{ext}} \cdot \partial_{\mathbf{k}} f_+ = \mathcal{C}_+ [f_+, f_-] \tag{101a}$$

$$\partial_t f_- + \mathbf{v}_- \cdot \partial_{\mathbf{r}} f_- + \mathbf{F}_-^{\text{ext}} \cdot \partial_{\mathbf{k}} f_- = \mathcal{C}_- [f_-, f_+] \tag{101b}$$

where the respective collision integrals $\mathcal{C}_+, \mathcal{C}_-$ are functionals in both f_+ and f_-. In this way, the two fluids couple only via interactions accounted for in the collision integrals.

As a first step, the above equations can be simplified by expanding around a local equilibrium. Specifically, a steady-state local equilibrium will be assumed where $T = T(\mathbf{r})$ may vary in space but the chemical potential μ is constant and there is no bulk flow: $\mathbf{V} = \mathbf{0}$. For electrons, such a state then reads

$$f_+^0(\mathbf{r}, \mathbf{k}) = \left(\exp\left(\frac{\epsilon_+(\mathbf{k}) - \mu}{k_B T(\mathbf{r})} \right) + 1 \right)^{-1} \tag{102}$$

For the holes, a slight re-definition of the distribution function f_- will be made to the left-hand side of its Boltzmann equation (101b). Namely, from the usual Fermi-Dirac-like distribution a filled band will be subtracted, corresponding to $f_- \to f_- - 1$. Since the left-hand side of the equation only contains derivatives, this leaves the overall equation unchanged. While not necessary for any of the calculations, this re-definition ensures the finiteness of quantities later encountered. From this re-definition, it follows that $f_- \leq 0$. In addition, the quantities from Section 3 must be adjusted; for instance, the number density of the holes is re-defined as

$$n_- \to \int \frac{\mathrm{d}^d k}{(2\pi)^d} \ (f_- - 1) \tag{103}$$

and similarly for the rest. Since then $n_- \leq 0$, it is natural to define a "charge" density

$$n_c = n_+ + n_- \tag{104}$$

which is positive when there are more electrons present than holes, and vice versa. This definition differs from the actual charge density by a factor of $-e$, but otherwise has the same properties. Similarly, an "imbalance" density could be defined by their difference:

$$n_{\text{imb}} = n_+ - n_- \tag{105}$$

which is then non-negative. Qualitatively, the imbalance density captures the number of excitations in the system. Thus, at finite temperature the imbalance density may be non-zero even at charge neutrality, where $n_c = 0$, due to thermal fluctuations.

The re-definition of f_- also implies that the local equilibrium distribution of the holes takes the form

$$\begin{aligned} f_-^0(\mathbf{r}, \mathbf{k}) &= \left(\exp\left(\frac{\epsilon_-(\mathbf{k}) - \mu}{k_B T(\mathbf{r})} \right) \right) - 1 \\ &= -\left(\exp\left(-\frac{\epsilon_-(\mathbf{k}) - \mu}{k_B T(\mathbf{r})} \right) + 1 \right)^{-1} \end{aligned} \tag{106}$$

Together, the two distributions can therefore be written

$$f_{\pm}^{0} = \pm \left(\exp\left(\pm \frac{\epsilon_{\pm} - \mu}{k_B T} \right) + 1 \right)^{-1} \tag{107}$$

having omitted the arguments. With this, the distributions $f_{\pm}$ are expanded around their local equilibrium states as

$$f_{+} = f_{+}^{0} + \delta f_{+} \tag{108a}$$
$$f_{-} = f_{-}^{0} + \delta f_{-} \tag{108b}$$

Under the assumptions on $T, \mu, \mathbf{V}$ above, the Boltzmann equations (101a) and (101b) then read

$$\partial_t \delta f_{+} + \partial_{\mathbf{k}} f_{+}^{0} \cdot \mathbf{F}_{+}^{\text{ext}} - \frac{\epsilon_{+} - \mu}{T} \partial_{\mathbf{k}} f_{+}^{0} \cdot \nabla T = \mathcal{C}_{+}\left[f_{+}, f_{-} \right] \tag{109a}$$
$$\partial_t \delta f_{-} + \partial_{\mathbf{k}} f_{-}^{0} \cdot \mathbf{F}_{-}^{\text{ext}} - \frac{\epsilon_{-} - \mu}{T} \partial_{\mathbf{k}} f_{-}^{0} \cdot \nabla T = \mathcal{C}_{-}\left[f_{-}, f_{+} \right] \tag{109b}$$

by comparison with (27). Moreover, the external forces present are assumed to arise due to an external electric field $\mathbf{E}$. This implies that the force terms read

$$\mathbf{F}_{+}^{\text{ext}} = -e\mathbf{E} \tag{110a}$$
$$\mathbf{F}_{-}^{\text{ext}} = -e\mathbf{E} \tag{110b}$$

where the fact that the force terms share the same sign, despite electrons and holes being oppositely charged, comes from the re-definition of the hole distribution f_{-}.

As the next step, the collision integrals are approximated in a way inspired by the relaxation time approximation. Explicitly, the scheme is

$$\mathcal{C}_{+}\left[f_{+}, f_{-} \right] = -\nu_{+-} \delta f_{+} + \nu_{-+} \delta f_{-} - \nu_{+}^{\text{dis}} \delta f_{+} \tag{111a}$$
$$\mathcal{C}_{-}\left[f_{-}, f_{+} \right] = -\nu_{-+} \delta f_{-} + \nu_{+-} \delta f_{+} - \nu_{-}^{\text{dis}} \delta f_{-} \tag{111b}$$

Here, the four rates $\nu_{+-}, \nu_{-+}, \nu_{+}^{\text{dis}}, \nu_{-}^{\text{dis}}$ are introduced, to capture different scattering processes accounted for. Firstly, ν_{+-} and ν_{-+} are related to electron-hole drag; that is, attractive Coulomb interactions between electrons and holes in graphene. In this way, the electron and hole fluids are able to exchange momentum with one another. In particular, the sign structure above ensures that total momentum is conserved between the two fluids, while momentum in each separate fluid is not necessarily conserved.

Next, the rates $\nu_{+}^{\text{dis}}, \nu_{-}^{\text{dis}}$ account for disorder scattering of the electrons and holes, respectively. In contrast to the Coulomb processes above, disorder scattering generally violates momentum conservation, and the corresponding terms of the collision integrals thus behave identically to that of (29). For simplicity, it will be assumed that these rates are equal for electrons and holes, i.e. $\nu_{+}^{\text{dis}} = \nu_{-}^{\text{dis}} := \nu^{\text{dis}}$.

It should be noted that this way of writing down a relaxation time-like approximation for the collision integrals is heuristic, and not derived from a formal approximation scheme. Neither does it specify exactly what scattering processes are being considered. Nonetheless, the different terms contained therein have the appropriate behaviour in regards to conservation laws, so these equations are expected to at least qualitatively describe the system. To provide a qualitative description is, however, as far as these equations realistically ought to be trusted, and the transport coefficients

obtained below are likely only correct to, say, within an order of magnitude. For a more exact treatment, either an improved approximation scheme or numerics are most likely needed.

Returning to the model at hand, the final step is to perform a temporal Fourier transform, which amounts to multiplying both sides of the equations by $e^{-i\omega t}$ followed by integrating over time. Since the local equilibrium state is assumed steady-state, the transform affects the deviations $\delta f_+, \delta f_-$ and the fields $\mathbf{E}, \nabla T$. To be fully precise, separate notation should be used for the Fourier transformed quantities when the arguments are being omitted, but for improved readability the same notation is used. Importantly, this Fourier transform sends the partial time derivative ∂_t to $-i\omega$ in the Boltzmann equations.

Inserting all of the above steps into the equations (109), one arrives at

$$-i\omega\delta f_+ - e\partial_{\mathbf{k}} f_+^0 \cdot \mathbf{E} - \frac{\epsilon_+ - \mu}{T}\partial_{\mathbf{k}} f_+^0 \cdot \nabla T = -\nu_{+-}\delta f_+ + \nu_{-+}\delta f_- - \nu_+^{\text{dis}}\delta f_+ \tag{112a}$$

$$-i\omega\delta f_- - e\partial_{\mathbf{k}} f_-^0 \cdot \mathbf{E} - \frac{\epsilon_- - \mu}{T}\partial_{\mathbf{k}} f_-^0 \cdot \nabla T = -\nu_{-+}\delta f_- + \nu_{+-}\delta f_+ - \nu_-^{\text{dis}}\delta f_- \tag{112b}$$

Importantly, the original coupled integro-differential equations have now been reduced to a system of linear equations in $\delta f_+, \delta f_-$, and can immediately be solved for these unknowns, in terms of the local equilibrium distributions and their derivatives. It is found that

$$\delta f_+ = \frac{\left(-i\omega + \nu^{\text{dis}} + \nu_{-+}\right)\left(e\partial_{\mathbf{k}} f_+^0 \cdot \mathbf{E} + \frac{\epsilon_+ - \mu}{T}\partial_{\mathbf{k}} f_+^0 \cdot \nabla T\right) + \nu_{-+}\left(e\partial_{\mathbf{k}} f_-^0 \cdot \mathbf{E} + \frac{\epsilon_- - \mu}{T}\partial_{\mathbf{k}} f_-^0 \cdot \nabla T\right)}{\left(-i\omega + \nu^{\text{dis}}\right)\left(-i\omega + \nu^{\text{dis}} + \nu_{+-} + \nu_{-+}\right)} \tag{113a}$$

$$\delta f_- = \frac{\left(-i\omega + \nu^{\text{dis}} + \nu_{+-}\right)\left(e\partial_{\mathbf{k}} f_-^0 \cdot \mathbf{E} + \frac{\epsilon_- - \mu}{T}\partial_{\mathbf{k}} f_-^0 \cdot \nabla T\right) + \nu_{+-}\left(e\partial_{\mathbf{k}} f_+^0 \cdot \mathbf{E} + \frac{\epsilon_+ - \mu}{T}\partial_{\mathbf{k}} f_+^0 \cdot \nabla T\right)}{\left(-i\omega + \nu^{\text{dis}}\right)\left(-i\omega + \nu^{\text{dis}} + \nu_{+-} + \nu_{-+}\right)} \tag{113b}$$

From these solutions, the resulting transport coefficients are found in the next section.

5.2 Transport Coefficients

To obtain the transport coefficients of the model, the electric and heat currents must first be related to the external fields as in (74). These currents, in turn, can be computed from the particle currents (34a) and energy currents (34b). Thus, the solutions (113) must be integrated over momentum, after first being multiplied by the appropriate functions.

5.2.1 Electrical Conductivity

Firstly, the particle currents are investigated, since these are related to the total electric current in the system, and thus the electrical conductivity. In this case, the Boltzmann equations are to be multiplied by $\mathbf{v}_\pm$ and then integrated. For notational convenience, a few short-hand terms for integrals are introduced:

$$\mathcal{E}_+ = -\int \frac{\mathrm{d}^d k}{(2\pi)^d}\, \mathbf{v}_+ \cdot \partial_{\mathbf{k}} f_+^0 \tag{114a}$$

$$\mathcal{E}_- = -\int \frac{\mathrm{d}^d k}{(2\pi)^d}\, \mathbf{v}_- \cdot \partial_{\mathbf{k}} f_-^0 \tag{114b}$$

and

$$\mathcal{T}_+ = -\int \frac{\mathrm{d}^d k}{(2\pi)^d} \frac{\epsilon_+ - \mu}{T} \mathbf{v}_+ \cdot \partial_{\mathbf{k}} f_+^0 \tag{115a}$$

$$\mathcal{T}_- = -\int \frac{\mathrm{d}^d k}{(2\pi)^d} \frac{\epsilon_- - \mu}{T} \mathbf{v}_- \cdot \partial_{\mathbf{k}} f_-^0 \tag{115b}$$

These could be called the "driving term integrals" of the system, and since they are integrals over the local equilibrium states they will, in general, be system-dependent. The reason for the global minus signs will become apparent once the transport coefficients are found.

With these definitions, the particle currents are found from (113) to be

$$\mathbf{j}_+ = -\frac{\left(-i\omega + \nu^{\mathrm{dis}} + \nu_{-+}\right)\left(e\mathcal{E}_+ \mathbf{E} + \mathcal{T}_+ \nabla T\right) - \nu_{-+}\left(e\mathcal{E}_- \mathbf{E} + \mathcal{T}_- \nabla T\right)}{\left(-i\omega + \nu^{\mathrm{dis}}\right)\left(-i\omega + \nu^{\mathrm{dis}} + \nu_{+-} + \nu_{-+}\right)} \tag{116a}$$

$$\mathbf{j}_- = -\frac{\left(-i\omega + \nu^{\mathrm{dis}} + \nu_{+-}\right)\left(e\mathcal{E}_- \mathbf{E} + \mathcal{T}_- \nabla T\right) - \nu_{+-}\left(e\mathcal{E}_+ \mathbf{E} + \mathcal{T}_+ \nabla T\right)}{\left(-i\omega + \nu^{\mathrm{dis}}\right)\left(-i\omega + \nu^{\mathrm{dis}} + \nu_{+-} + \nu_{-+}\right)} \tag{116b}$$

In the above process, the particle-hole symmetry $\epsilon_-(\mathbf{k}) = -\epsilon_+(\mathbf{k})$ of graphene is necessary to evaluate a few arising "mixed" integrals. The particle-hole symmetry implies

$$\mathbf{v}_- = \partial_{\mathbf{k}} \epsilon_- = -\partial_{\mathbf{k}} \epsilon_+ = -\mathbf{v}_+ \tag{117}$$

With this, integrals such as

$$\begin{aligned} -\int \frac{\mathrm{d}^d k}{(2\pi)^d}\, \mathbf{v}_- \cdot \partial_{\mathbf{k}} f_+^0 &= \int \frac{\mathrm{d}^d k}{(2\pi)^d}\, \mathbf{v}_+ \cdot \partial_{\mathbf{k}} f_+^0 \\ &= -\mathcal{E}_+ \end{aligned} \tag{118}$$

can be evaluated. The total electric current $\mathbf{j}^{\mathrm{el}}$ is then given by the sum of the currents above, multiplied by $-e$. Since their sum involves sums and differences of the driving term integrals, it is again convenient to introduce shorthand notation, to the same end as the "charge" and imbalance densities were introduced in (103) and (104), respectively. Thus, one writes

$$\mathcal{E}_c = \mathcal{E}_+ + \mathcal{E}_- \tag{119a}$$

$$\mathcal{E}_{\mathrm{imb}} = \mathcal{E}_+ - \mathcal{E}_- \tag{119b}$$

$$\mathcal{T}_c = \mathcal{T}_+ + \mathcal{T}_- \tag{119c}$$

$$\mathcal{T}_{\mathrm{imb}} = \mathcal{T}_+ - \mathcal{T}_- \tag{119d}$$

Finally, it so happens that the rates ν_{+-}, ν_{-+} only appear in terms of their sums and difference, motivating some final definitions

$$\nu_+ = \nu_{+-} + \nu_{-+} \tag{120a}$$

$$\nu_- = \nu_{+-} - \nu_{-+} \tag{120b}$$

With these, the electric current is found to be

$$\begin{aligned} \mathbf{j}^{\mathrm{el}} &= -e\left(\mathbf{j}_+ + \mathbf{j}_-\right) \\ &= \left(\frac{e^2\mathcal{E}_c + \frac{\nu_-}{\nu_+} e^2 \mathcal{E}_{\mathrm{imb}}}{-i\omega + \nu_+} - \frac{\nu_-}{\nu_+} \frac{e^2 \mathcal{E}_{\mathrm{imb}}}{-i\omega + \nu^{\mathrm{dis}}}\right) \mathbf{E} \\ &\quad - \left(\frac{e\mathcal{T}_c + \frac{\nu_-}{\nu_+} e\mathcal{T}_{\mathrm{imb}}}{-i\omega + \nu_+} - \frac{\nu_-}{\nu_+} \frac{e\mathcal{T}_{\mathrm{imb}}}{-i\omega + \nu^{\mathrm{dis}}}\right) \nabla T \end{aligned} \tag{121}$$

where a *hydrodynamic regime* has been assumed, so that $\nu_+ \gg \nu^{\text{dis}}$. From the above expression, the DC electrical conductivity can be immediately read off as

$$\sigma_{DC}(\mu, T) = \frac{e^2\mathcal{E}_c + \frac{\nu_-}{\nu_+}e^2\mathcal{E}_{\text{imb}}}{\hbar\nu_+} - \frac{\nu_-}{\nu_+}\frac{e^2\mathcal{E}_{\text{imb}}}{\hbar\nu^{\text{dis}}} \tag{122}$$

where the arguments μ, T are made explicit to remind the reader that both the scattering rates and the driving term integrals depend, in general, both on the chemical potential and the temperature. Also, the factor of $\hbar$ has been restored from dimensional analysis.

In particular, at the charge neutrality point $\mu = 0$ it must be required that $\nu_{+-} = \nu_{-+}$, so that $\nu_- = 0$. Moreover, it is found that

$$f_-^0 = -f_+^0 \tag{123}$$

due to particle-hole symmetry. This implies that $\mathcal{E}_{\text{imb}} = 0$, and the resulting electrical conductivity at charge neutrality is

$$\sigma_{DC}(\mu = 0, T) = \frac{e^2\mathcal{E}_c}{\hbar\nu_+} \tag{124}$$

This result is thus in agreement with other theoretical findings [48, 41, 21], reporting a minimal conductivity of graphene at charge neutrality. Strikingly, the electrical conductivity at the charge neutrality point remains finite, even in the clean limit $\nu^{\text{dis}} \to 0$. This result may appear counter-intuitive, in that there (at a first glance) appears to be no mechanism of momentum relaxation present in the system when disorder is removed. In such a case, the usual arguments from, say, Drude theory would indicate that the electrical conductivity must diverge. However, there is an intuitive argument for why this does not occur in graphene, which can be appealed to with the aid of the schematic shown in Figure 7. Firstly, the relation $f_-^0 = -f_+^0$ implies that there are equal densities of electrons and holes at the charge neutrality point. Moreover, an applied electric field will accelerate the electrons and holes in exactly opposite directions, due to their opposite charge. Since the two particle types also have the same mass, the net rate at which momentum is induced in the system by the electric field is zero. In view of this, it is perhaps reasonable that momentum relaxation via disorder is not needed to maintain a finite electrical conductivity. Instead, the Coulomb drag between electrons and phonons regulate the electric current induced by the field.

Away from charge neutrality, it is seen from (122) that the conductivity does diverge in the clean limit $\nu^{\text{dis}} \to 0$. In light of the above, this can be understood by noting that the densities of electrons and holes are no longer equal, so that a net momentum *is* induced over time by an applied electric field. This creates the need for a momentum relaxation mechanism, in this case provided by disorder.

Finally, it can be shown that the minimal conductivity is non-negative in graphene, given the isotropy of the phonon dispersion (99). This is done in Appendix B, as well as showing the non-negativity of the remaining transport coefficients found in the following sections.

5.2.2 Thermal Conductivity

To obtain the thermal conductivity, the above steps must be reproduced, only that (instead) the Boltzmann equations are multiplied by $\epsilon_\pm \mathbf{v}_\pm$ before integration. Again, it is helpful to make some

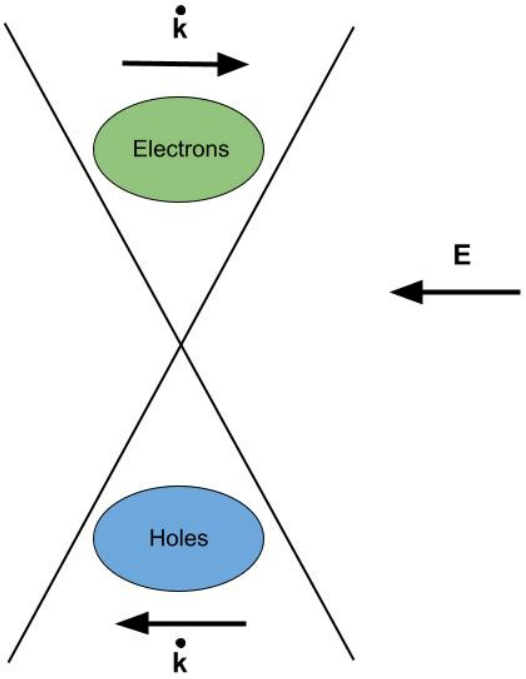

Figure 7: Schematic of the response of graphene at charge neutrality to an electric field **E**. Here, the equal "clouds" of electrons and holes are accelerated in opposite directions, and no net momentum is induced over time.

shorthand definitions

$$\mathcal{E}^{\epsilon}_{+} = -\int \frac{\mathrm{d}^d k}{(2\pi)^d}\, \epsilon_{+}\mathbf{v}_{+}\cdot\partial_{\mathbf{k}} f^0_{+} \tag{125a}$$

$$\mathcal{E}^{\epsilon}_{-} = -\int \frac{\mathrm{d}^d k}{(2\pi)^d}\, \epsilon_{-}\mathbf{v}_{-}\cdot\partial_{\mathbf{k}} f^0_{-} \tag{125b}$$

$$\mathcal{T}^{\epsilon}_{+} = -\int \frac{\mathrm{d}^d k}{(2\pi)^d}\, \epsilon_{+}\frac{\epsilon_{+}-\mu}{T}\mathbf{v}_{+}\cdot\partial_{\mathbf{k}} f^0_{+} \tag{125c}$$

$$\mathcal{T}^{\epsilon}_{-} = -\int \frac{\mathrm{d}^d k}{(2\pi)^d}\, \epsilon_{+}\frac{\epsilon_{-}-\mu}{T}\mathbf{v}_{-}\cdot\partial_{\mathbf{k}} f^0_{-} \tag{125d}$$

along with their respective sums and differences

$$\mathcal{E}^{\epsilon}_{c} = \mathcal{E}^{\epsilon}_{+} + \mathcal{E}^{\epsilon}_{-} \tag{126a}$$

$$\mathcal{E}^{\epsilon}_{\mathrm{imb}} = \mathcal{E}^{\epsilon}_{+} - \mathcal{E}^{\epsilon}_{-} \tag{126b}$$

$$\mathcal{T}^{\epsilon}_{c} = \mathcal{T}^{\epsilon}_{+} + \mathcal{T}^{\epsilon}_{-} \tag{126c}$$

$$\mathcal{T}^{\epsilon}_{\mathrm{imb}} = \mathcal{T}^{\epsilon}_{+} - \mathcal{T}^{\epsilon}_{-} \tag{126d}$$

This time, the energy currents are found to be

$$\mathbf{j}_+^\epsilon = -\frac{\left(-i\omega+\nu^{\text{dis}}+\nu_{-+}\right)\left(e\mathcal{E}_+^\epsilon\mathbf{E}+\mathcal{T}_+^\epsilon\nabla T\right)+\nu_{-+}\left(e\mathcal{E}_-^\epsilon\mathbf{E}+\mathcal{T}_-^\epsilon\nabla T\right)}{\left(-i\omega+\nu^{\text{dis}}\right)\left(-i\omega+\nu^{\text{dis}}+\nu_{+-}+\nu_{-+}\right)} \tag{127a}$$

$$\mathbf{j}_-^\epsilon = -\frac{\left(-i\omega+\nu^{\text{dis}}+\nu_{+-}\right)\left(e\mathcal{E}_-^\epsilon\mathbf{E}+\mathcal{T}_-^\epsilon\nabla T\right)+\nu_{+-}\left(e\mathcal{E}_+^\epsilon\mathbf{E}+\mathcal{T}_+^\epsilon\nabla T\right)}{\left(-i\omega+\nu^{\text{dis}}\right)\left(-i\omega+\nu^{\text{dis}}+\nu_{+-}+\nu_{-+}\right)} \tag{127b}$$

Notably, the "mixed" integrals do not give rise a sign change like (118), since the integrands are now multiplied by

$$\epsilon_\pm\mathbf{v}_\pm = \epsilon_\mp\mathbf{v}_\mp \tag{128}$$

It follows that the total heat current is given by

$$\begin{aligned}\mathbf{j}^q &= \left(\mathbf{j}_+^\epsilon+\mathbf{j}_-^\epsilon\right)-\mu\left(\mathbf{j}_++\mathbf{j}_-\right)\\ &= -\left(\frac{e\mathcal{E}_c^\epsilon-\frac{\mu\nu_-}{\nu_+}e\mathcal{E}_{\text{imb}}}{-i\omega+\nu^{\text{dis}}}-\mu\frac{e\mathcal{E}_c-\frac{\nu_-}{\nu_+}e\mathcal{E}_{\text{imb}}}{-i\omega+\nu_+}\right)\mathbf{E}\\ &\quad-\left(\frac{\mathcal{T}_c^\epsilon-\frac{\mu\nu_-}{\nu_+}\mathcal{T}_{\text{imb}}}{-i\omega+\nu^{\text{dis}}}-\mu\frac{\mathcal{T}_c-\frac{\nu_-}{\nu_+}\mathcal{T}_{\text{imb}}}{-i\omega+\nu_+}\right)\nabla T\end{aligned} \tag{129}$$

With this, the general expression for the thermal conductivity κ can be calculated, but the result is rather lengthy. Instead, the conductivity at charge neutrality is investigated, in which case the expression reduces to

$$\kappa(\mu=0,T) = \frac{\mathcal{T}_c^\epsilon}{\hbar\nu^{\text{dis}}} \tag{130}$$

for static fields, i.e. $\omega = 0$. In contrast to the electrical conductivity, κ does diverge in the clean limit $\nu^{\text{dis}} \to 0$. This can be physically argued via a schematic similar to Figure 7, given in Figure 8. Like before, there are equal densities of electrons and holes at charge neutrality. However, an applied thermal gradient ∇T has the same effect on both fluids, so that the rate at which net momentum is induced is non-zero. Whereas electron-hole drag was sufficient to render σ finite, it is perhaps natural that disorder is needed as a momentum relaxation mechanism for κ to not diverge.

6 Electron-Hole-Phonon Description

6.1 Model

In this section, phonons are incorporated into the model (101). This amounts to adding a third equation for a third fluid, labelled by b since the constituent particles have Bose-Einstein statistics. Thus, the most general model takes on the form

$$\partial_t f_+ + \mathbf{v}_+\cdot\partial_{\mathbf{r}} f_+ + \mathbf{F}_+^{\text{ext}}\cdot\partial_{\mathbf{k}} f_+ = \mathcal{C}_+\left[f_+, f_-, b\right] \tag{131a}$$

$$\partial_t f_- + \mathbf{v}_-\cdot\partial_{\mathbf{r}} f_- + \mathbf{F}_-^{\text{ext}}\cdot\partial_{\mathbf{k}} f_- = \mathcal{C}_-\left[f_-, f_+, b\right] \tag{131b}$$

$$\partial_t b + \mathbf{v}_b\cdot\partial_{\mathbf{r}} b + \mathbf{F}_b^{\text{ext}}\cdot\partial_{\mathbf{k}} b = \mathcal{C}_b\left[b, f_+, f_-\right] \tag{131c}$$

where the respective collision integrals $\mathcal{C}_+, \mathcal{C}_-, \mathcal{C}_b$ generally couple all three fluids with one another. At this point, all the steps done in Section 5.1 will be repeated with only a few adjustments, notably regarding the collision integrals. The relevant observations are summarised below.

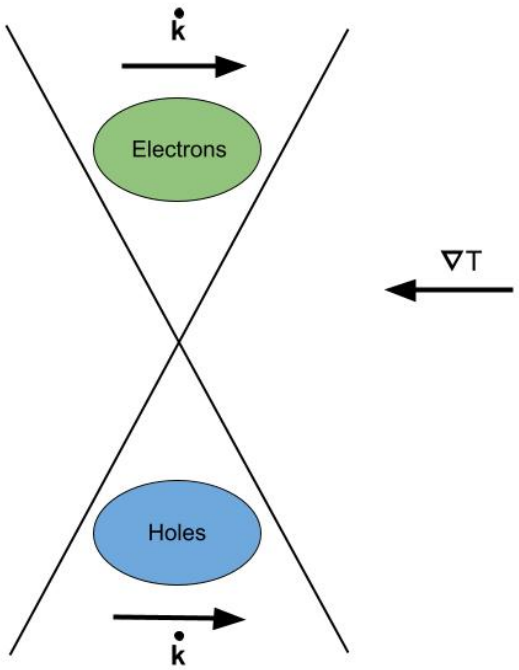

Figure 8: Schematic of the response of graphene at charge neutrality to a thermal gradient ∇T. This time, the equal "clouds" of electrons and holes are accelerated in the same direction, resulting in a non-zero net momentum induced over time.

Since phonons are charge neutral, they are unaffected by the electric field, so that

$$\mathbf{F}_b^{\text{ext}} = \mathbf{0} \tag{132}$$

Moreover, the local equilibrium distribution describing the phonons is of the Bose-Einstein form, i.e.

$$b^0(\mathbf{r}, \mathbf{k}) = \left(\exp\left(\frac{\epsilon_b(\mathbf{k})}{k_B T(\mathbf{r})} \right) - 1 \right)^{-1} \tag{133}$$

Then, an expansion $b = b^0 + \delta b$ around local equilibrium yields

$$\partial_t b = \partial_t \delta b \tag{134a}$$

$$\mathbf{v}_b \cdot \partial_{\mathbf{r}} b \approx \mathbf{v}_b \cdot \partial_{\mathbf{r}} b^0 = -\frac{\epsilon_b}{T} \partial_{\mathbf{k}} b^0 \cdot \nabla T \tag{134b}$$

Next, a temporal Fourier transform only changes $\partial_t \delta b \to -i\omega \delta b$.

Importantly, the relaxation time approximation scheme for the collision integrals must be updated. This time, they are written in the form

$$\mathcal{C}_+ [f_+, f_-, b] = -\nu_{+-} \delta f_+ + \nu_{-+} \delta f_- - \nu^{\text{dis}} \delta f_+ - \nu_{+b} \delta f_+ + \nu_{b+} \delta b \tag{135a}$$

$$\mathcal{C}_- [f_-, f_+, b] = -\nu_{-+} \delta f_- + \nu_{+-} \delta f_+ - \nu^{\text{dis}} \delta f_- - \nu_{-b} \delta f_- + \nu_{b-} \delta b \tag{135b}$$

$$\mathcal{C}_b [b, f_+, f_-] = -\nu_b \delta b - \nu_{b+} \delta b - \nu_{b-} \delta b + \nu_{+b} \delta f + \nu_{-b} \delta f_- \tag{135c}$$

The rates $\nu_{+-}, \nu_{-+}, \nu^{\text{dis}}$ from Section 5.1 still remain, with the same interpretations, and a few additional rates are introduced here. Firstly, ν_{+b} and ν_{b+} refer to collisions of electrons and phonons. Again, the relaxation time approximation does not specify exactly what processes are being described, but for graphene these would typically be processes where an electron collides with an atom and either absorbs or emits a phonon. Like for the electron-hole drag, the sign structure above ensures conservation of momentum and energy in these collisions. Similarly, ν_{-b} and ν_{b-} refer to collisions between holes and phonons, with analogous properties. Lastly, ν_b is associated with conservation-violating processes for phonons. These could include disorder scattering and/or Umklapp scattering, and generally provide a mechanism for momentum relaxation of the phonon fluid, even for vanishing interaction strengths between phonons and electrons/holes.

With all of the above modifications, the Boltzmann equations now read

$$-i\omega\delta f_+ - e\partial_{\mathbf{k}} f_+^0 \cdot \mathbf{E} - \frac{\epsilon_+ - \mu}{T}\partial_{\mathbf{k}} f_+^0 \cdot \nabla T = -\nu_{+-}\delta f_+ + \nu_{-+}\delta f_- - \nu^{\text{dis}}\delta f_+ - \nu_{+b}\delta f_+ + \nu_{b+}\delta b \tag{136a}$$

$$-i\omega\delta f_- - e\partial_{\mathbf{k}} f_-^0 \cdot \mathbf{E} - \frac{\epsilon_- - \mu}{T}\partial_{\mathbf{k}} f_-^0 \cdot \nabla T = -\nu_{-+}\delta f_- + \nu_{+-}\delta f_+ - \nu^{\text{dis}}\delta f_- - \nu_{-b}\delta f_- + \nu_{b-}\delta b \tag{136b}$$

$$-i\omega\delta b - \frac{\epsilon_b}{T}\partial_{\mathbf{k}} b^0 \cdot \nabla T = -\nu_b\delta b - \nu_{b+}\delta b - \nu_{b-}\delta b + \nu_{+b}\delta f + \nu_{-b}\delta f_- \tag{136c}$$

In the same way, the original Boltzmann equations become a set of linear equations in $\delta f_+, \delta f_-, \delta b$, and can in principle be solved for the distributions.

6.2 Transport Coefficients

Because the solutions of the above equations are quite lengthy, charge neutrality will be assumed from here on. On the one hand, this drastically simplifies the expressions since (in addition to the observations made in Section 5.2 and its subsections) it follows that $\nu_{b+} = \nu_{b-}$ and $\nu_{+b} = \nu_{-b}$. At the same, the charge neutrality point offers the transport behaviour that is most unique to Dirac materials.

6.2.1 Electrical Conductivity

Like before, the Boltzmann equations (136) are first to be multiplied by the respective velocities $\mathbf{v}_\pm, \mathbf{v}_b$ and then integrated over momentum. In addition to the previously defined driving term integrals, a few more are needed for the phononic integral

$$\mathcal{T}_b = -\int \frac{\mathrm{d}^d k}{(2\pi)^d}\ \frac{\epsilon_b}{T}\mathbf{v}_b \cdot \partial_{\mathbf{k}} \tag{137}$$

as well as some mixed integrals

$$\mathcal{T}_{\pm,b} = -\int \frac{\mathrm{d}^d k}{(2\pi)^d}\ \mathbf{v}_\pm \cdot \frac{\epsilon_b}{T}\partial_{\mathbf{k}} b^0 \tag{138a}$$

$$\mathcal{E}_{b,\pm} = -\int \frac{\mathrm{d}^d k}{(2\pi)^d}\ \mathbf{v}_b \cdot \partial_{\mathbf{k}} f_\pm^0 \tag{138b}$$

$$\mathcal{T}_{b,\pm} = -\int \frac{\mathrm{d}^d k}{(2\pi)^d}\ \mathbf{v}_b \cdot \frac{\epsilon_\pm - \mu}{T}\partial_{\mathbf{k}} f_\pm^0 \tag{138c}$$

These integrals, like their counterparts in the electron-hole description of Section 5.2.1, are generally system-dependent, since they depend on the local-equilibrium distributions $f^0_\pm, b^0$. Also, like before, terms containing $\pm$ indices always combine into their sums and differences, so immediately one defines

$$\mathcal{T}_{c,b} = \mathcal{T}_{+,b} + \mathcal{T}_{-,b} \tag{139a}$$
$$\mathcal{T}_{\text{imb},b} = \mathcal{T}_{+,b} - \mathcal{T}_{-,b} \tag{139b}$$
$$\mathcal{E}_{b,c} = \mathcal{E}_{b,+} + \mathcal{E}_{b,-} \tag{139c}$$
$$\mathcal{E}_{b,\text{imb}} = \mathcal{E}_{b,+} - \mathcal{E}_{b,-} \tag{139d}$$
$$\mathcal{T}_{b,c} = \mathcal{T}_{b,+} + \mathcal{T}_{b,-} \tag{139e}$$
$$\mathcal{T}_{b,\text{imb}} = \mathcal{T}_{b,+} - \mathcal{T}_{b,-} \tag{139f}$$

and note that charge neutrality implies

$$\mathcal{T}_{c,b} = \mathcal{E}_{b,c} = \mathcal{T}_{b,\text{imb}} = 0 \tag{140}$$

Going through the resulting calculations, the total electric current is found to be

$$\begin{aligned}\mathbf{j}^{\text{el}} &= -e\left(\mathbf{j}_+ + \mathbf{j}_-\right) + 0\mathbf{j}_b \\ &= \frac{e^2\mathcal{E}_c}{-i\omega + \nu^{\text{dis}} + \nu_{+b} + \nu_+}\mathbf{E}\end{aligned} \tag{141}$$

Therefore, the DC conductivity is read off as (with the factor of $\hbar$ re-inserted)

$$\sigma_{DC}(\mu = 0, T) = \frac{e^2\mathcal{E}_c}{\hbar\left(\nu_{+b} + \nu_+\right)} \tag{142}$$

in the hydrodynamic regime $\nu_+ \gg \nu^{\text{dis}}$. Much like the conductivity found in 5.2.1, this electrical conductivity remains finite in the clean limit $\nu^{\text{dis}} \to 0$; in other words, the minimal conductivity persists when phonons are included in the description. This is reasonable, as phonons would be expected to have a minimal impact on electric properties of the system, given their neutral electric charge. Indeed, the expression for σ above differs only from that of (124) by the presence of the term ν_{+b} in the denominator, which amounts to a slight reduction of the conductivity. Considering that electrons and holes are able to "lose" momentum to the phonons, which do not contribute to the electric current, the result agrees with physical intuition.

6.2.2 Thermal Conductivity

Following the same steps of defining more driving term integrals and then performing the integration, one defines

$$\mathcal{T}^\epsilon_b = -\int \frac{\mathrm{d}^d k}{(2\pi)^d}\, \epsilon_b \mathbf{v}_b \cdot \frac{\epsilon_b}{T}\partial_{\mathbf{k}} b^0 \tag{143a}$$
$$\mathcal{T}^\epsilon_{\pm,b} = -\int \frac{\mathrm{d}^d k}{(2\pi)^d}\, \epsilon_\pm \mathbf{v}_\pm \cdot \frac{\epsilon_b}{T}\partial_{\mathbf{k}} b^0 \tag{143b}$$
$$\mathcal{E}^\epsilon_{b,\pm} = -\int \frac{\mathrm{d}^d k}{(2\pi)^d}\, \epsilon_b \mathbf{v}_b \cdot \partial_{\mathbf{k}} f^0_\pm \tag{143c}$$
$$\mathcal{T}^\epsilon_{b,\pm} = -\int \frac{\mathrm{d}^d k}{(2\pi)^d}\, \epsilon_b \mathbf{v}_b \cdot \frac{\epsilon_\pm - \mu}{T}\partial_{\mathbf{k}} f^0_\pm \tag{143d}$$

along with their sums and differences

$$\mathcal{T}^{\epsilon}_{c,b} = \mathcal{T}^{\epsilon}_{+,b} + \mathcal{T}^{\epsilon}_{-,b} \tag{144a}$$
$$\mathcal{T}^{\epsilon}_{\mathrm{imb},b} = \mathcal{T}^{\epsilon}_{+,b} - \mathcal{T}^{\epsilon}_{-,b} \tag{144b}$$
$$\mathcal{E}^{\epsilon}_{b,c} = \mathcal{E}^{\epsilon}_{b,+} + \mathcal{E}^{\epsilon}_{b,-} \tag{144c}$$
$$\mathcal{E}^{\epsilon}_{b,\mathrm{imb}} = \mathcal{E}^{\epsilon}_{b,+} - \mathcal{E}^{\epsilon}_{b,-} \tag{144d}$$
$$\mathcal{T}^{\epsilon}_{b,c} = \mathcal{T}^{\epsilon}_{b,+} + \mathcal{T}^{\epsilon}_{b,-} \tag{144e}$$
$$\mathcal{T}^{\epsilon}_{b,\mathrm{imb}} = \mathcal{T}^{\epsilon}_{b,+} - \mathcal{T}^{\epsilon}_{b,-} \tag{144f}$$

where charge neutrality asserts that

$$\mathcal{T}^{\epsilon}_{\mathrm{imb},b} = \mathcal{E}^{\epsilon}_{b,c} = \mathcal{T}^{\epsilon}_{b,\mathrm{imb}} = 0 \tag{145}$$

After having found the total heat current, which in fact is equal to the total energy current as $\mu = 0$ at charge neutrality, the thermal conductivity for static fields (i.e. for $\omega = 0$) is found to be

$$\kappa(\mu = 0, T) = \frac{(\nu_b + 2\nu_{b+})\,\mathcal{T}^{\epsilon}_{c} + 2\nu_{b+}\mathcal{T}^{\epsilon}_{c,b} + \left(\nu^{\mathrm{dis}} + \nu_{+b}\right)\mathcal{T}^{\epsilon}_{b} + \nu_{+b}\mathcal{T}^{\epsilon}_{b,c}}{\hbar\left(2\nu_{b+}\nu^{\mathrm{dis}} + \nu_b\left(\nu^{\mathrm{dis}} + \nu_{+b}\right)\right)} \tag{146}$$

This expression varies drastically from the one obtained in (130), which is not surprising given that it was argued in Section 4.1.2 that phonons ought to greatly impact the thermal conductivity. However, it is less clear under which circumstances κ is finite, and it is therefore instructive to consider a few different limits. It is found that the conductivity always diverges if three or more of the scattering rates $\nu^{\mathrm{dis}}, \nu_{b+}, \nu_{+b}, \nu_b$ vanish, and also that the conductivity remains finite in the limit of any one rate vanishing. This leaves the limits of two vanishing rates, where it is found that only three of the six possible limits yield a finite result. These are

$$\lim_{(\nu_{b+},\nu_{+b})\to(0,0)} \kappa = \frac{\mathcal{T}^{\epsilon}_{c}}{\hbar\nu^{\mathrm{dis}}} + \frac{\mathcal{T}^{\epsilon}}{\hbar\nu_b} \tag{147a}$$
$$\lim_{(\nu_b,\nu_{+b})\to(0,0)} \kappa = \frac{\mathcal{T}^{\epsilon}_{c} + \mathcal{T}^{\epsilon}_{c,b}}{\hbar\nu^{\mathrm{dis}}} + \frac{\mathcal{T}^{\epsilon}_{b}}{2\hbar\nu_{b+}} \tag{147b}$$
$$\lim_{(\nu^{\mathrm{dis}},\nu_{b+})\to(0,0)} \kappa = \frac{\mathcal{T}^{\epsilon}_{c}}{\hbar\nu_{+b}} + \frac{\mathcal{T}^{\epsilon}_{b} + \mathcal{T}^{\epsilon}_{b,c}}{\hbar\nu_b} \tag{147c}$$

The finiteness of the above limits again agree with intuition. In (169), electron-phonon and hole-phonon interactions are both negligible. Thus, the electrons and holes must be able to "lose" momentum on their own, and similarly for the phonons. Thus, it would be expected that the thermal conductivity diverges if either $\nu^{\mathrm{dis}} \to 0$ or $\nu_b \to 0$. In (173), $\nu_b \to 0$ indicates that the phonons have no mechanism for momentum relaxation on their own. Instead, the conductivity remains finite because electrons and holes have such a mechanism, together with the fact that phonons are able to "lose" momentum to electrons/holes. In (174), the situation is reversed, where phonons have momentum relaxation on their own, and electrons/holes are able to "lose" momentum to the phonons.

7 Outlook

There are many directions in which this thesis project could be continued. The most obvious one would be to use a more exact expression for the collision integrals. This would certainly produce

more accurate results, but would likely make the resulting equations impossible to solve analytically, meaning one would have to resort to numerics.

This aside, the (somewhat of a) lack of of comparisons with data in Sections 5 and 6 should be addressed. This could be remedied either by performing simulations, or by comparison with experiment. As for simulations, there was simply not enough time near the end of this thesis project to consider running simulations, but this would certainly be an interesting direction to immediately test the validity of the two models used. As for experiments, quantities like the minimal electrical conductivity remain elusive. However, comparisons with the expressions for the transport coefficients are difficult regardless since they involve integrals over the local equilibrium distributions, meaning they must be calculated for the specific system investigated. At the same time, this could be considered a strength of the models; since their formulation is so general, they should be expected to qualitatively describe any Dirac material. In fact, the only graphene-specific assumption used was the fact that the phononic dispersion was isotropic in $\mathbf{k}$. In addition, although the model was developed with phonons in mind, the third bosonic fluid in (131c) could really represent any bosons. In another materials, it may instead assume the role of, say, other collective modes such as plasmons, or different bosons altogether, adding to the generality of the model.

Another direction to consider is the temperature-dependence of the transport coefficients found. While some of the driving term integrals already have factors of temperature inserted in their definitions, all of the scattering rates in the relaxation time approximation schemes will also generally carry a temperature dependence. This could potentially open up for different regimes where different rates in the system dominate, which would have the largest impact on the thermal conductivity where the scattering rates enter in various combinations. It might also add additional nuance to the "phase diagram" of graphene reported by e.g. [49].

In addition, the models used fail to account for a few interactions expected to also impact the transport coefficients. For instance, electron-electron and hole-hole interactions are not accounted for, but are certainly present due to Coulomb interactions. Such interactions would also be crucial to include when considering viscosities in the system, which is yet another direction to consider. However, the relaxation time approximation cannot describe e.g. electron-electron interactions in a way that preserves particle number, momentum and energy. Therefore, a different approach must be taken to solving the Boltzmann equations when considering these interactions.

There are many other corrections that could be considered. One effect which does not change the model, but which alters the driving term integrals, is to improve the method for finding the spectrum of graphene, $\epsilon_{\pm}$. While a nearest-neighbour tight-binding model like (82) captures the essential properties of graphene, it incorrectly describes a linear spectrum up to energy/temperature scales on the order of

$$T = \frac{t}{k_B} \approx 10^5 \text{ K} \tag{148}$$

A more accurate analysis reveals that the spectrum displays non-linearity much earlier, with the Fermi velocity depending quite significantly on the charge carrier densities [50].

8 Summary

This thesis started off by introducing the Boltzmann equation in Section 2 as a tool to study transport in condensed matter systems via a hydrodynamic description. It is one of few theories able to describe many-body systems that are driven out of equilibrium. In addition, it is non-perturbative in particle interaction strength, and is therefore applicable to quantum systems where e.g. electron-electron interactions are non-negligible. Moreover, due to its integro-differential nature, various

approximation methods were introduced to be able to obtain analytical results, notably through the relaxation time approximation.

Following this, a framework for transport theory was set up in Section 3 using the Boltzmann equation, and it was shown how the Boltzmann equation integrates to give three equations of fluid dynamics, each representing a conservation law. Moreover, the Onsager reciprocal relations were discussed, allowing for a simplification in the analysis of the different transport coefficients.

After this, Dirac materials were introduced in Section 4, which are a class of materials unified by their quasiparticles having a "relativistic" dispersion, described by the Dirac equation. These materials are all strongly interacting, and share many properties that separate them from e.g. ordinary metals. A few examples were discussed explicitly, such as the conservation of chirality leading to the Klein paradox, or how the common mass of the particles and antiparticles described is directly connected to the band gap of the system. In particular, graphene was seen to be an excellent candidate for observing electron hydrodynamics in. This was due largely to the fact that ultraclean samples can be produced in the lab, as well as electron-electron interactions in graphene being two orders of magnitude stronger than those of quantum electrodynamics, allowing for a hydrodynamic regime where Coulomb interactions dominate disorder and phonon scattering.

Having established the setting, two models for graphene were developed. In the first, given in Section 5, only electrons and holes were considered, resulting in two coupled Boltzmann equations. These were solved by introducing a relaxation time-like approximation scheme, which ensured that particle momentum and energy were conserved in electron-hole interactions, while allowing for conservation-violating disorder scattering. These equations were then solved, and the thermoelectric transport coefficients were found. Firstly, the electrical conductivity σ was found to have a non-zero value at the charge neutrality point, in agreement with other so-called minimal electrical conductivities reported for graphene. The electrical conductivity was also found to remain finite, even in the clean limit. This was explained by noting that an applied electric field does not induce a net momentum in the electron-hole system, due to the particle-hole symmetry of Dirac materials. Instead, Coulomb drag between the electron and the hole fluids is enough to maintain a finite conductivity. Secondly, the thermal conductivity κ was found, which was observed to diverge in the clean limit. This was understood by noting that a thermal gradient does induce a net momentum in the electron-hole system, leading to the necessity of momentum relaxation via disorder.

After this, the second model for graphene was introduced in Section 6, including phonons as a third fluid. The relaxation time approximation scheme above was generalised to incorporate also electron-phonon and hole-phonon interactions, as well as phononic interactions that violate conservation laws. Then, the transport coefficients were re-derived. The electrical conductivity was found to be mostly unchanged, which could be understood by noting that phonons do not contribute to the electric current. Nonetheless, a slight reduction of σ was noted, which can be argued to occur due to the "loss" of momentum of electrons/holes to the phonons. The finding for κ did, however, significantly vary from the expression found in the first model. This was to be expected from considerations of phonons in graphene. The thermal conductivity was found to remain finite only for specific limits, which were understood in terms of the separate momentum relaxation mechanisms of electrons/holes and phonons separately, as well as the interplay between the two.

Finally, an outlook was presented in Section 7, discussing various areas of improvement, as well as possible future directions of research.

References

[1] A. E. Evrard, F. J. Summers, and M. Davis. "Two-fluid simulations of galaxy formation". In: *Astrophys. J.* 422.1 (1994), pp. 11–36.

[2] G. Stadler et al. "The Dynamics of Plate Tectonics and Mantle Flow: From Local to Global Scales". In: *Science* 329.5995 (2010), pp. 1033–1038.

[3] J. L. Silverberg et al. "Collective Motion of Humans in Mosh and Circle Pits at Heavy Metal Concerts". In: *Phys. Rev. Lett.* 110 (22 2013), p. 228701.

[4] N. W. Ashcroft and N. D. Mermin. *Solid State Physics*. Harcourt College Publishers, 1976. ISBN: 0-03-083993-9.

[5] O. Klein. "Die Reflexion von Elektronen an einem Potentialsprung nach der relativistischen Dynamik von Dirac". In: *Z. Phys.* 53.3 (1929), pp. 157–165.

[6] K. S. Novoselov et al. "Electric Field Effect in Atomically Thin Carbon Films". In: *Science* 306.5696 (2004), pp. 666–669.

[7] E. M. Lifshitz and L. P. Pitaevskii. *Course of Theoretical Physics: Vol. 10 Physical Kinetics*. Pergamon Press Ltd., 1981. Chap. 1, pp. 4–17. ISBN: 0-08-020641-7.

[8] S. Weinstock. "Boltzmann collision term". In: *Phys. Rev. D* 73 (2 2006), p. 025005.

[9] A. Lucas and K. C. Fong. "Hydrodynamics of Electrons in Graphene". In: *J. Phys. Condens. Matter* 30.5 (2018), p. 053001.

[10] P. L. Bhatnagar, E. P. Gross, and M. Krook. "A Model for Collision Processes in Gases. I. Small Amplitude Processes in Charged and Neutral One-Component Systems". In: *Phys. Rev.* 94 (3 1954), pp. 511–525.

[11] E. P. Gross. "Plasma Oscillations in a Static Magnetic Field". In: *Phys. Rev.* 82 (2 1951), pp. 232–242.

[12] G. S. Rocha, G. S. Denicol, and J. Noronha. "Novel Relaxation Time Approximation to the Relativistic Boltzmann Equation". In: *Phys. Rev. Lett.* 127 (4 2021), p. 042301.

[13] S. Bhadury et al. "Relaxation-time approximation with pair production and annihilation processes". In: *Phys. Rev. C* 102 (6 2020), p. 064910.

[14] S. R. De Groot and P. Mazur. *Non-Equilibrium Thermodynamics*. Dover Publications, 2013. Chap. 4, pp. 35–40. ISBN: 0-486-64741-2.

[15] J. M. Ziman. *Electrons and Phonons*. Clarendon Press, 1960. Chap. 7.

[16] T. O. Wehling, A. M. Black-Schaffer, and A. V. Balatsky. "Dirac materials". In: *Adv. Phys.* 63.1 (2014), pp. 1–76.

[17] P. A. M. Dirac. "The quantum theory of the electron". In: *Proc. R. Soc. A* 117.778 (1928), pp. 610–624.

[18] M. I. Katsnelson and K. S. Novoselov. "Graphene: New bridge between condensed matter physics and quantum electrodynamics". In: *Solid State Commun.* 143.1-2 (2007), pp. 3–13.

[19] S. Yue et al. "Observation of one-dimensional Dirac fermions in silicon nanoribbons". In: *Nano Lett.* 22.2 (2022), pp. 695–701.

[20] T. Ando, T. Nakanishi, and R. Saito. "Berry's Phase and Absence of Back Scatteringin Carbon Nanotubes". In: *J. Phys. Soc. Jpn.* 67.8 (1998), pp. 2857–2862.

[21] A. H. Castro Neto et al. "The electronic properties of graphene". In: *Rev. Mod. Phys.* 81 (1 2009), pp. 109–162.

[22] C. C. Tsuei and J. R. Kirtley. "Pairing symmetry in cuprate superconductors". In: *Rev. Mod. Phys.* 72 (4 2000), pp. 969–1016.

[23] A. K. Geim and K. S. Novoselov. "The rise of graphene". In: *Nat. Mater.* 6 (2007), pp. 183–191.

[24] P. R. Wallace. "The Band Theory of Graphite". In: *Phys. Rev.* 6 (9 1947), pp. 622–634.

[25] J. C. Slonczewski and P. R. Weiss. "Band Structure of Graphite". In: *Phys. Rev.* 109 (2 1958), pp. 272–279.

[26] E. Fradkin. "Critical behavior of disordered degerenate semiconductors. II. Spectrum and transport properties in mean-field theory". In: *Phys. Rev. B* 33 (5 1986), pp. 3263–3268.

[27] R. Peierls. "Quelques propriétés des corps solides". In: *Ann. I. H. Poincaré* 5 (3 1935), pp. 177–222.

[28] N. D. Mermin. "Crystalline Order in Two Dimensions". In: *Phys. Rev.* 176 (1 1968), pp. 250–254.

[29] J. C. Meyer et al. "The structure of suspended graphene sheets". In: *Nature* 446 (2007), pp. 60–63.

[30] R. C. Thompson-Flagg, M. J. B. Moura, and M. Marder. "Rippling of graphene". In: *EPL* 85.4 (2009), p. 46002.

[31] D. Huertas-Hernando, F. Guinea, and A. Brataas. "Spin-orbit coupling in curved graphene, fullerenes, nanotubes, and nanotube caps". In: *Phys. Rev. B* 74 (15 2006), p. 155426.

[32] Y. Yao et al. "Spin-orbit gap of graphene: First-principles calculations". In: *Phys. Rev. B* 75 (4 2007), p. 041401.

[33] G. Dresselhaus and M. S. Dresselhaus. "Spin-Orbit Interaction in Graphite". In: *Phys. Rev.* 140 (1A 1965), A401–A412.

[34] Y. Hasegawa et al. "Zero modes of tight-binding electrons on the honeycomb lattice". In: *Phys. Rev. B* 74 (3 2006), p. 033413.

[35] J.-H. Chen et al. "Charged-impurity scattering in graphene". In: *Nat. Phys.* 4 (2008), pp. 377–381.

[36] S. Samaddar et al. "Charge Puddles in Graphene near the Dirac Point". In: *Phys. Rev. Lett.* 116 (12 2016), p. 126804.

[37] Q. Su et al. "Ultraclean Graphene Transfer Using a Sacrificial Fluoropolymer Nanolayer: Implications for Sensor and Electronic Applications". In: *ACS Appl. Nano Matter* 3 (12 2020), pp. 11998–12007.

[38] L. Zheng et al. "Robust ultraclean atomically thin membranes for atomic-resolution electron microscopy". In: *Nat. Commun.* 11.541 (2020).

[39] J. A. Sulpizio et al. "Visualizing Poiseuille flow of hydrodynamic electons". In: *Nature* 576 (2019), pp. 75–79.

[40] D. A. Bandurin et al. "Negative local resistance caused by viscous electron backflow in graphene". In: *Science* 351.6277 (2016), pp. 1055–1058.

[41] K. S. Novoselov et al. "Two-dimensional gas of massless Dirac fermions in graphene". In: *Nature* 438 (2005), pp. 197–200.

[42] N. M. Gabor et al. “Hot Carrier-Assisted Intrinsic Photoresponse in Graphene”. In: *Science* 334.6056 (2011), pp. 648–652.

[43] L. Fritz et al. “Quantum critical transport in clean graphene”. In: *Phys. Rev. B* 78 (8 2008), p. 085416.

[44] N. M. R. Peres. “Colloquium: The transport properties of graphene: An introduction”. In: *Rev. Mod. Phys.* 82 (3 2010), pp. 2673–2700.

[45] K. C. Fong and K. C. Schwab. “Ultrasensitive and Wide-Bandwidth Thermal Measurements of Graphene at Low Temperatures”. In: *Phys. Rev. X* 2 (3 2012), p. 031006.

[46] K. Komatsu and T. Nagamiya. “Theory of the Specific Heat of Graphite”. In: *J. Phys. Soc. Jpn.* 6.6 (1951), pp. 438–444.

[47] K. Komatsu. “Theory of the Specific Heat of Graphite II”. In: *J. Phys. Soc. Jpn.* 10.5 (1955), pp. 346–356.

[48] L. Moriconi and D. Niemeyer. “Graphene conductivity near the charge neutral point”. In: *Phys. Rev. B* 84 (19 2011), p. 193401.

[49] D. E. Sheehy and J. Schmalian. “Quantum Critical Scaling in Graphene”. In: *Phys. Rev. Lett.* 99 (22 2007), p. 226803.

[50] D. C. Elias et al. “Dirac cones reshaped by interaction effects in suspended graphene”. In: *Nat. Phys.* 7 (2011), pp. 701–704.

Appendix A: Collisional Invariants

In this appendix, it is shown how the conservation laws of the collisions that enter the collision integral are reflected in the vanishing of momentum integrals over the collision integral. Specifically, this will be shown for 2-body interactions resulting in a collision integral of the form (12). However, these properties transfer to general n-body scattering events in a natural way.

As the starting point, one considers integrals of the form

$$\int \mathrm{d}^d p\ \varphi \mathcal{C}[f]$$

for some general function $\varphi = \varphi(\mathbf{r}, \mathbf{p}, t)$. Such an integral expresses how the density of the quantity φ evolves in time due to collisions in the system. In particular, if the above integral vanishes, φ is said to be a *collisional invariant*. Explicitly, this integral reads

$$\int \mathrm{d}^d p\ \varphi \mathcal{C}[f] = \int \mathrm{d}p \mathrm{d}^d p_1 \mathrm{d}^d p' \mathrm{d}^d p'_1\ w\left(\mathbf{p}, \mathbf{p}_1 | \mathbf{p}', \mathbf{p}'_1\right) \varphi \left(f' f'_1 - f f_1\right) \tag{149}$$

Now, since all four momenta are integrated over, one may freely re-name them into each other to obtain

$$\int \mathrm{d}^d p\ \varphi \mathcal{C}[f] = \int \mathrm{d}^d p \mathrm{d}^d p_1 \mathrm{d}^d p' \mathrm{d}^d p'_1\ w\left(\mathbf{p}, \mathbf{p}_1 | \mathbf{p}', \mathbf{p}'_1\right) f' f'_1 \left(\varphi - \varphi'\right) \tag{150}$$

where the same index notation is used for φ as it is for f, so that e.g. $\varphi' = \varphi(\mathbf{r}, \mathbf{p}', t)$. Next, since w is related to the probability of a scattering rate, it is invariant under the swapping of the ingoing particles and/or the outgoing ones. This is to say,

$$w\left(\mathbf{p}_1, \mathbf{p} | \mathbf{p}', \mathbf{p}'_1\right) = w\left(\mathbf{p}, \mathbf{p}_1 | \mathbf{p}', \mathbf{p}'_1\right) = w\left(\mathbf{p}, \mathbf{p}_1 | \mathbf{p}'_1, \mathbf{p}'\right) \tag{151}$$

With this, the expression (150) can be written

$$\int \mathrm{d}^d p\ \varphi \mathcal{C}[f] = \frac{1}{2} \int \mathrm{d}^d p \mathrm{d}^d p_1 \mathrm{d}^d p' \mathrm{d}^d p'_1\ w\left(\mathbf{p}, \mathbf{p}_1 | \mathbf{p}', \mathbf{p}'_1\right) f' f'_1 \left(\varphi + \varphi_1 - \varphi' - \varphi'_1\right) \tag{152}$$

Now, φ is conserved in collisions precisely when $\varphi + \varphi_1 = \varphi' + \varphi'_1$, or equivalently when

$$\varphi + \varphi_1 - \varphi' - \varphi'_1 = 0 \tag{153}$$

Thus, the conservation of φ in collisions implies that

$$\int \mathrm{d}^d p\ \varphi \mathcal{C}[f] = 0 \tag{154}$$

In particular, there are three choices of φ which highlight central conservation laws. Firstly, there is $\varphi = 1$, which is certainly conserved since $1 + 1 - 1 - 1 = 0$. This corresponds to the conservation of particle number, which is already assumed in writing down the collision integral (12), so this is no surprise. Explicitly, inserting $\varphi = 1$ gives

$$\int \mathrm{d}^d p\ \mathcal{C}[f] = 0 \tag{155}$$

which is (45).

Secondly, one could consider $\varphi = p_i$, i.e. letting φ denote a component of the momentum. Then, if the collision process conserve momentum, it follows that $\mathbf{p} + \mathbf{p}' = \mathbf{p}' + \mathbf{p}_1'$, which in particular holds for each component of the momentum. Therefore,

$$\int \mathrm{d}^d p \; p_i \mathcal{C}[f] = 0 \tag{156}$$

Adding together these different components gives the vector relation which is

$$\int \mathrm{d}^d p \; \mathbf{p} \mathcal{C}[f] = \mathbf{0} \tag{157}$$

expressing momentum conservation in integral form. This is precisely (51).

Finally, a third choice is $\varphi = \epsilon$. Provided energy is conserved in collisions, i.e. $\epsilon + \epsilon_1 = \epsilon' + \epsilon_1'$, the analogous relation

$$\int \mathrm{d}^d p \; \epsilon \mathcal{C}[f] = 0 \tag{158}$$

holds, which is the final equation (54).

Interestingly, there is one more conserved quantity that can be found. Detailed balance implies that the (local) equilibrium distribution f^0 satisfies

$$f^0 f_1^0 = f^{0\prime} f^{0\prime}{}_1 \tag{159}$$

so as to make the collision integral vanish when evaluated on a (local) equilibrium solution: $\mathcal{C}\left[f^0\right] = 0$. Taking the logarithm on both sides yields

$$\ln\left(f^0\right) + \ln\left(f_1^0\right) = \ln\left(f^{0\prime}\right) + \ln\left(f^{0\prime}{}_1\right) \tag{160}$$

which shows that $\varphi = \ln\left(f^0\right)$ is in fact also a collisional invariant. Specifically, if particle number, momentum, and energy are the only three independent conserved quantities, then $\ln\left(f^0\right)$ must be expressible as a linear combination of those. In its most general form, this reads

$$\ln\left(f^0\right) = -\frac{\epsilon}{k_B T} + \frac{\mu}{k_B T} + \frac{\mathbf{p} \cdot \mathbf{V}}{k_B T} \tag{161}$$

for some parameters $T, \mu, \mathbf{V}$ which may possibly depend on space and time, but not momentum. Exponentiating both sides gives

$$f^0 = \exp\left(-\frac{\epsilon - \mu - \mathbf{p} \cdot \mathbf{V}}{k_B T}\right) \tag{162}$$

which is exactly the Boltzmann distribution. In this way, the parameters $T, \mu, \mathbf{V}$ correspond precisely to the notation used earlier, namely the temperature, chemical potential, and bulk flow profile, respectively. This derivation therefore shows that the collision integral, derived for classical particles, enforces the Boltzmann distribution as the equilibrium solution. Similarly, the Fermi-Dirac and Bose-Einstein distributions can be derived by appealing to the (quantum) collision integral (16). In these cases, the appropriate collisional invariant to consider is

$$\varphi = \ln\left(\frac{f^0}{1 \mp f^0}\right) \tag{163}$$

Appendix B: Non-Negativity of the Transport Coefficients

This appendix is devoted to showing the non-negativity of the transport coefficients found in Sections 5 and 6.

In the expressions for the electrical conductivity found in (124) and (142) at charge neutrality, the driving integral term appearing is $\mathcal{E}_c$, which by particle-hole symmetry satisfies $\mathcal{E}_c = 2\mathcal{E}_+$. By definition,

$$\mathcal{E}_+ = -\int \frac{\mathrm{d}^d k}{(2\pi)^d}\ \mathbf{v}_+ \cdot \partial_{\mathbf{k}} f_+^0 \tag{164}$$

For graphene, or Dirac materials more generally, the velocity $\mathbf{v}_+$ is provided by its dispersion as

$$\mathbf{v}_+ = \frac{\partial \epsilon_+}{\partial \mathbf{k}} = v_F \hat{\mathbf{k}} \tag{165}$$

where $\hat{\mathbf{k}}$ is a unit vector pointing in the direction of $\mathbf{k}$, i.e. $\hat{\mathbf{k}} = \frac{\mathbf{k}}{|\mathbf{k}|}$. Moreover, f_+^0 is a local Fermi-Dirac distribution of the form

$$\begin{aligned} f_+^0(\mathbf{r}, \mathbf{k}) &= \left(\exp\left(\frac{\epsilon_+(\mathbf{k})}{T}\right)\right)^{-1} \\ &= \left(\exp\left(\frac{v_F|\mathbf{k}|}{T}\right) + 1\right)^{-1} \end{aligned} \tag{166}$$

Therefore,

$$\partial_{\mathbf{k}} f_+^0 = -\left(\exp\left(\frac{v_F|\mathbf{k}|}{T}\right) + 1\right)^{-2} \exp\left(\frac{v_F|\mathbf{k}|}{T}\right) \frac{v_F}{T}\hat{\mathbf{k}} \tag{167}$$

which, in turn, implies

$$\begin{aligned} \mathcal{E}_c &= -\int \frac{\mathrm{d}^d k}{(2\pi)^d}\ v_F\hat{\mathbf{k}} \cdot \left(-\left(\exp\left(\frac{v_F|\mathbf{k}|}{T}\right) + 1\right)^{-2} \exp\left(\frac{v_F|\mathbf{k}|}{T}\right) \frac{v_F}{T}\hat{\mathbf{k}}\right) \\ &= \frac{2v_F^2}{T}\int \frac{\mathrm{d}^d k}{(2\pi)^d}\ \left(\exp\left(\frac{v_F|\mathbf{k}|}{T}\right) + 1\right)^{-2} \exp\left(\frac{v_F|\mathbf{k}|}{T}\right) \end{aligned} \tag{168}$$

In particular, the integrand is now strictly positive, implying that $\mathcal{E}_c > 0$. Thus, the conductivity is strictly positive in both models, as was the claim.

For the thermal conductivity (130) in the electron-hole model, $\mathcal{T}_c^\epsilon$ must similarly be investigated. This time, similar reasoning yields

$$\begin{aligned} \mathcal{T}_c^\epsilon &= 2\mathcal{T}_+^\epsilon \\ &= \frac{2v_F^2}{T^2}\int \frac{\mathrm{d}^d k}{(2\pi)^d}\ \epsilon_+ \left(\exp\left(\frac{v_F|\mathbf{k}|}{T}\right) + 1\right)^{-2} \exp\left(\frac{v_F|\mathbf{k}|}{T}\right) \\ &> 0 \end{aligned} \tag{169}$$

where the integrand is again positive because ϵ_+ is. Thus, κ is positive in the electron-hole model.

When phonons are considered, resulting in (146) for the thermal conductivity, there are three more driving term integrals to consider, namely $\mathcal{T}_{c,b}^\epsilon$, $\mathcal{T}_b^\epsilon$, and $\mathcal{T}_{b,c}^\epsilon$. This time, a more explicit phononic

dispersion ϵ_b is needed, and for this any of the three modes in (99) could be used. Importantly, they are all functions in the magnitude of the momentum $|\mathbf{k}|$, or in other words isotropic in the momentum. They are also all increasing functions in $|\mathbf{k}|$. It follows that

$$\begin{aligned}\mathbf{v}_b \cdot \hat{\mathbf{k}} &= \partial_{\mathbf{k}} \epsilon_b \cdot \hat{\mathbf{k}} \\ &= \partial_{|\mathbf{k}|} \epsilon_b \hat{\mathbf{k}} \cdot \hat{\mathbf{k}} \\ &> 0\end{aligned} \tag{170}$$

and

$$\begin{aligned}\partial_{\mathbf{k}} b^0 \cdot \hat{\mathbf{k}} &= -\left(\exp\left(\frac{\epsilon_b}{T}\right) - 1\right)^{-2} \exp\left(\frac{\epsilon_b}{T}\right) \frac{1}{T} \partial_{\mathbf{k}} \epsilon_b \cdot \hat{\mathbf{k}} \\ &< 0\end{aligned} \tag{171}$$

Moreover,

$$\mathbf{v}_b \cdot \partial_{\mathbf{k}} b^0 < 0 \tag{172}$$

by combining the above two relations. Therefore,

$$\begin{aligned}\mathcal{T}_b^{\epsilon} &= -\int \frac{\mathrm{d}^d k}{(2\pi)^d} \, \epsilon_b \mathbf{v}_b \cdot \frac{\epsilon_b}{T} \partial_{\mathbf{k}} b^0 \\ &= -\frac{1}{T} \int \frac{\mathrm{d}^d k}{(2\pi)^d} \, \epsilon_b^2 \mathbf{v}_b \cdot \partial_{\mathbf{k}} b^0 \\ &> 0\end{aligned} \tag{173}$$

Next,

$$\begin{aligned}\mathcal{T}_{c,b}^{\epsilon} &= 2\mathcal{T}_{+,b}^{\epsilon} \\ &= -2 \int \frac{\mathrm{d}^d k}{(2\pi)^2} \, \epsilon_+ \mathbf{v}_+ \cdot \frac{\epsilon_b}{T} \partial_{\mathbf{k}} b^0 \\ &= -\frac{2 v_F^2}{T} \int \frac{\mathrm{d}^d k}{(2\pi)^2} \, |\mathbf{k}| \epsilon_b \partial_{|\mathbf{k}|} b^0 \\ &> 0\end{aligned} \tag{174}$$

because $\partial_{|\mathbf{k}|} b^0 < 0$, by virtue of (171). Finally,

$$\begin{aligned}\mathcal{T}_{b,c}^{\epsilon} &= 2\mathcal{T}_{b,+}^{\epsilon} \\ &= -2 \int \mathrm{d}^2 k \, \epsilon_b \mathbf{v}_b \cdot \frac{\epsilon_+}{T} \partial_{\mathbf{k}} f_+^0 \\ &= -\frac{2}{T} \int \frac{\mathrm{d}^d k}{(2\pi)^d} \epsilon_b \partial_{|\mathbf{k}|} \epsilon_b \hat{\mathbf{k}} \cdot \partial_{\mathbf{k}} f_+^0 \\ &> 0\end{aligned} \tag{175}$$

for the same reasons as in (168), i.e. $\hat{\mathbf{k}} \cdot \partial_{\mathbf{k}} f_+^0 < 0$. Together, (169), (173), (174), and (175) indicate that the thermal conductivity found in (146) is, in fact, also positive.